

Validation of the Aura Microwave Limb Sounder HNO₃ measurements

M. L. Santee,¹ A. Lambert,¹ W. G. Read,¹ N. J. Livesey,¹ R. E. Cofield,¹ D. T. Cuddy,¹ W. H. Daffer,¹ B. J. Drouin,¹ L. Froidevaux,¹ R. A. Fuller,¹ R. F. Jarnot,¹ B. W. Knosp,¹ G. L. Manney,^{1,2} V. S. Perun,¹ W. V. Snyder,¹ P. C. Stek,¹ R. P. Thurstans,¹ P. A. Wagner,¹ J. W. Waters,¹ G. Muscari,³ R. L. de Zafra,⁴ J. E. Dibb,⁵ D. W. Fahey,⁶ P. J. Popp,^{6,7} T. P. Marcy,^{6,7,8} K. W. Jucks,⁹ G. C. Toon,¹ R. A. Stachnik,¹ P. F. Bernath,^{10,11} C. D. Boone,¹⁰ K. A. Walker,^{10,12} J. Urban,¹³ and D. Murtagh¹³

Received 29 March 2007; revised 4 September 2007; accepted 12 October 2007; published 28 December 2007.

[1] We assess the quality of the version 2.2 (v2.2) HNO₃ measurements from the Microwave Limb Sounder (MLS) on the Earth Observing System Aura satellite. The MLS HNO₃ product has been greatly improved over that in the previous version (v1.5), with smoother profiles, much more realistic behavior at the lowest retrieval levels, and correction of a high bias caused by an error in one of the spectroscopy files used in v1.5 processing. The v2.2 HNO₃ data are scientifically useful over the range 215 to 3.2 hPa, with single-profile precision of ~0.7 ppbv throughout. Vertical resolution is 3–4 km in the upper troposphere and lower stratosphere, degrading to ~5 km in the middle and upper stratosphere. The impact of various sources of systematic uncertainty has been quantified through a comprehensive set of retrieval simulations. In aggregate, systematic uncertainties are estimated to induce in the v2.2 HNO₃ measurements biases that vary with altitude between ±0.5 and ±2 ppbv and multiplicative errors of ±5–15% throughout the stratosphere, rising to ~±30% at 215 hPa. Consistent with this uncertainty analysis, comparisons with correlative data sets show that relative to HNO₃ measurements from ground-based, balloon-borne, and satellite instruments operating in both the infrared and microwave regions of the spectrum, MLS v2.2 HNO₃ mixing ratios are uniformly low by 10–30% throughout most of the stratosphere. Comparisons with in situ measurements made from the DC-8 and WB-57 aircraft in the upper troposphere and lowermost stratosphere indicate that the MLS HNO₃ values are low in this region as well, but are useful for scientific studies (with appropriate averaging).

Citation: Santee, M. L., et al. (2007), Validation of the Aura Microwave Limb Sounder HNO₃ measurements, *J. Geophys. Res.*, 112, D24S40, doi:10.1029/2007JD008721.

1. Introduction

[2] Nitric acid (HNO₃) is a key atmospheric constituent. As a central participant in both the activation and the deactivation of chlorine, HNO₃ indirectly regulates the magnitude, spatial extent, and duration of ozone destruction in the stratosphere [e.g., Solomon, 1999; Santee *et al.*, 1999,

2004, and references therein]. It is also a primary reservoir for reactive nitrogen and a major player in processes controlling ozone abundances and clouds in the upper troposphere [e.g., Crutzen *et al.*, 1999; Zondlo *et al.*, 2000, and references therein].

¹Jet Propulsion Laboratory, California Institute of Technology, Pasadena, California, USA.

²Also at Department of Physics, New Mexico Institute of Mining and Technology, Socorro, New Mexico, USA.

³Istituto Nazionale di Geofisica e Vulcanologia, Rome, Italy.

⁴Department of Physics and Astronomy, and Institute for Terrestrial and Planetary Atmospheres, State University of New York, Stony Brook, New York, USA.

⁵Climate Change Research Center, Institute for the Study of Earth, Oceans, and Space, University of New Hampshire, Durham, New Hampshire, USA.

Copyright 2007 by the American Geophysical Union.
0148-0227/07/2007JD008721

⁶Chemical Sciences Division, Earth System Research Laboratory, NOAA, Boulder, Colorado, USA.

⁷Also at Cooperative Institute for Research in Environmental Sciences, University of Colorado, Boulder, Colorado, USA.

⁸Now at Milwaukee, Wisconsin, USA.

⁹Harvard-Smithsonian Center for Astrophysics, Cambridge, Massachusetts, USA.

¹⁰Department of Chemistry, University of Waterloo, Waterloo, Ontario, Canada.

¹¹Now at Department of Chemistry, University of York, York, UK.

¹²Now at Department of Physics, University of Toronto, Toronto, Ontario, Canada.

¹³Department of Radio and Space Science, Chalmers University of Technology, Göteborg, Sweden.

[3] The Microwave Limb Sounder (MLS) on NASA's Earth Observing System (EOS) Aura satellite measures vertical profiles of HNO₃ globally on a daily basis. Initial validation of the first publicly available Aura MLS HNO₃ data set, version 1.5 (v1.5), was presented by *Froidevaux et al.* [2006] and *Barret et al.* [2006]. Here we report on the quality of the recently released version 2.2 (v2.2) Aura MLS HNO₃ measurements. The measurement system is described in section 2. In addition to providing a review of instrumental and orbital characteristics, this section includes guidelines for quality control that should be applied to the v2.2 HNO₃ measurements, documents their precision and spatial resolution, and quantifies sources of systematic uncertainty. Because the v1.5 Aura MLS HNO₃ data have been featured in some previous studies [e.g., *Schoeberl et al.*, 2006a; *Santee et al.*, 2005], section 2 also provides an overview of the differences between v2.2 and v1.5 HNO₃. In section 3, "zeroth-order" validation of the Aura MLS HNO₃ data is accomplished by comparing against climatological averages in narrow equivalent-latitude bands compiled from the multiyear Upper Atmosphere Research Satellite (UARS) MLS HNO₃ data set. Accuracy is assessed through comparisons with correlative data sets from a variety of platforms in section 4. Finally, in section 5 we summarize the Aura MLS v2.2 HNO₃ validation results.

2. Aura MLS HNO₃ Measurement Description

2.1. Overview of the MLS Measurement System

[4] Aura, the last in NASA's EOS series of satellites, was launched on 15 July 2004 into a near-polar, Sun-synchronous, 705-km altitude orbit with a 1345 local time (LT) ascending equator-crossing time [*Schoeberl et al.*, 2006b]. One of its four instruments, Aura MLS, is an advanced successor to the Microwave Limb Sounder on UARS. Detailed information on the microwave limb sounding technique in general and the Aura MLS instrument in particular is given by *Waters* [1993] and *Waters et al.* [2006], respectively. MLS observes a large suite of atmospheric parameters by measuring millimeter- and submillimeter-wavelength thermal emission from Earth's limb with seven radiometers covering five broad spectral regions. Nitric acid is measured by three of the radiometers: those centered near 190, 240, and 640 GHz. The standard HNO₃ product is derived from the 240-GHz retrievals at and below (i.e., at pressures equal to or larger than) 10 hPa and from the 190-GHz retrievals above that level; the HNO₃ measurements from the 640-GHz radiometer have significantly poorer precision and are not considered further here.

[5] The Aura MLS fields of view point forward in the direction of orbital motion and vertically scan the limb in the orbit plane, leading to data coverage from 82°S to 82°N latitude on every orbit. Thus Aura MLS obtains continuous daily sampling of both polar regions, with none of the temporal gaps from yaw maneuvers that occurred with UARS MLS. The MLS limb scans are synchronized to the Aura orbit, with 240 scans per orbit at essentially fixed latitudes. This results in ~3500 scans per day, with an along-track separation between adjacent retrieved profiles of 1.5° great circle angle (~165 km). The longitudinal separation of MLS measurements, set by the Aura orbit, is 10°–20° over low and middle latitudes, with much finer

sampling in the polar regions. Most MLS data products, including HNO₃, are reported on a fixed vertical pressure grid with six levels per decade change in pressure in the troposphere and stratosphere.

[6] The MLS "Level 2" data (retrieved geophysical parameters and diagnostics at the measurement locations along the suborbital track) are generated from input "Level 1" data (calibrated radiances and engineering information) by the MLS data processing software. The MLS retrieval algorithms, described in detail by *Livesey et al.* [2006], are based on the standard optimal estimation method; they employ a two-dimensional approach that takes into account the fact that limb observations from consecutive scans cover significantly overlapping regions of the atmosphere. The data are divided into overlapping "chunks" consisting of the measurements in a 15° span of great circle angle (typically about 10 vertical profiles); retrievals are performed for each of these chunks independently and then joined together to produce a complete set of output [*Livesey et al.*, 2006]. The results are reported in Level 2 Geophysical Product (L2GP) files, which are standard HDF-EOS version 5 files containing swaths in the Aura-wide standard format [*Livesey et al.*, 2007a]. A separate L2GP file is produced for each standard MLS product for each day (0000–2400 UT).

[7] Reprocessing with the v2.2 algorithms of the MLS data collected to date is ongoing; however, at the time of writing (February 2007) only a small subset of the data, consisting of fewer than 100 d, has been reprocessed, with priority given to days for which correlative measurements exist. Although small compared to the entire MLS data record, this set of v2.2 days spans all seasons and is sufficient for thorough investigation of the MLS data quality.

2.2. MLS HNO₃ Data Usage Guidelines

[8] Along with the data fields, the L2GP files contain corresponding precision fields, which quantify the impact of radiance noise on the data and, particularly in regions with less measurement sensitivity, the contribution of a priori information. The data processing software flags the precision with a negative sign when the estimated precision is worse than 50% of the a priori precision; thus only data points for which the associated precision value is positive should be used.

[9] Three additional data quality metrics are provided for every vertical profile of each product. "Status" is a bit field indicating operational abnormalities or problems with the retrievals; see Table 1 for a complete description. Profiles for which "Status" is an odd number should not be used in any scientific study. Nonzero but even values of "Status" indicate that the profile has been marked as questionable, typically because the measurements may have been affected by the presence of thick clouds (see section 2.5). Globally ~10–15% of profiles are identified in this manner, with the fraction of profiles possibly impacted by clouds rising to ~25–35% on average in the tropics. Clouds generally have little influence on the stratospheric HNO₃ data. In the lowermost stratosphere and upper troposphere, however, thick clouds can lead to artificial enhancements in the HNO₃ mixing ratios in the equatorial regions. Therefore it is recommended that at and below 100 hPa all profiles with

Table 1. Meaning of Bits in the “Status” Field

Bit	Value ^a	Meaning
0	1	flag: do not use this profile (see bits 8–9 for details)
1	2	flag: this profile is “suspect” (see bits 4–6 for details)
2	4	unused
3	8	unused
4	16	information: this profile may have been affected by high-altitude clouds
5	32	information: this profile may have been affected by low-altitude clouds
6	64	information: this profile did not use GEOS-5 temperature a priori data
7	128	unused
8	256	information: retrieval diverged or too few radiances available for retrieval
9	512	information: the task retrieving data for this profile crashed (typically a computer failure)

^a“Status” field in L2GP file is total of appropriate entries in this column.

nonzero values of “Status” be used with extreme caution or discarded altogether because of the potential for cloud contamination. This is a blunt tool that has the unfortunate consequence of rejecting many profiles that are probably not significantly impacted by cloud effects; further investigation as more v2.2 data become available may help to refine this cloud screening procedure.

[10] The “Quality” field describes the degree to which the measured MLS radiances have been fitted by the Level 2 algorithms. In theory, larger values of “Quality” indicate generally good radiance fits, whereas values closer to zero indicate poorer radiance fits and thus less reliable data. In practice, low values of “Quality” are not always associated with profiles that are obviously “bad.” As a precaution, we recommend rejecting profiles having “Quality” values less than 0.4. This threshold for “Quality” typically excludes $\sim 2\text{--}3\%$ of HNO₃ profiles on a daily basis; it is a conser-

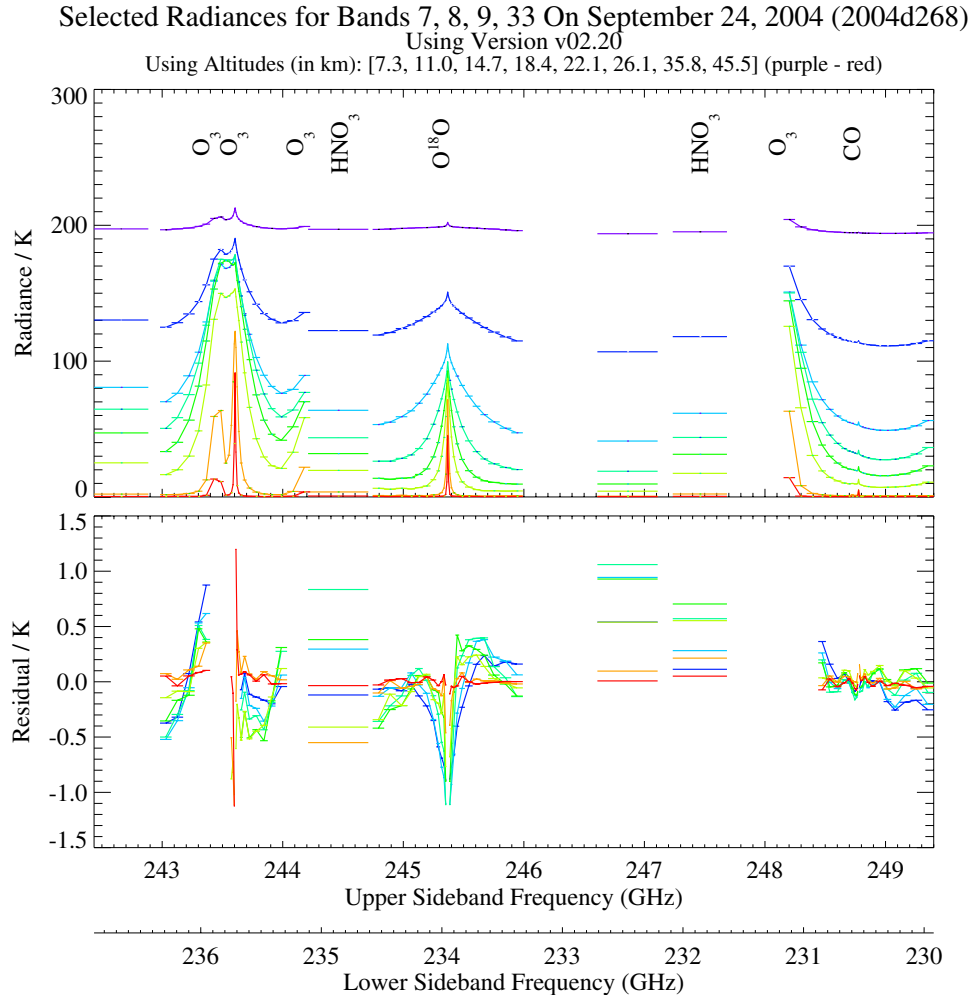


Figure 1. Sample radiances and residuals from the Aura MLS 240-GHz radiometer for bands 7–9 and 33. (top) Global average radiances for a representative day (24 September 2004), expressed as brightness temperature (in K), for eight selected tangent point altitudes from 7.3 km (purple) to 45.5 km (red). The MLS signal is a combination of incoming radiance at frequencies above (upper sideband, upper x axis) and below (lower sideband, lower x axis) the 239.660 GHz local oscillator. The widths of the various MLS spectral channels are denoted by the horizontal bars. (bottom) Average residual of the fit achieved by the MLS version 2.2 retrieval algorithms. Residuals for channels not used in the retrievals are not shown.

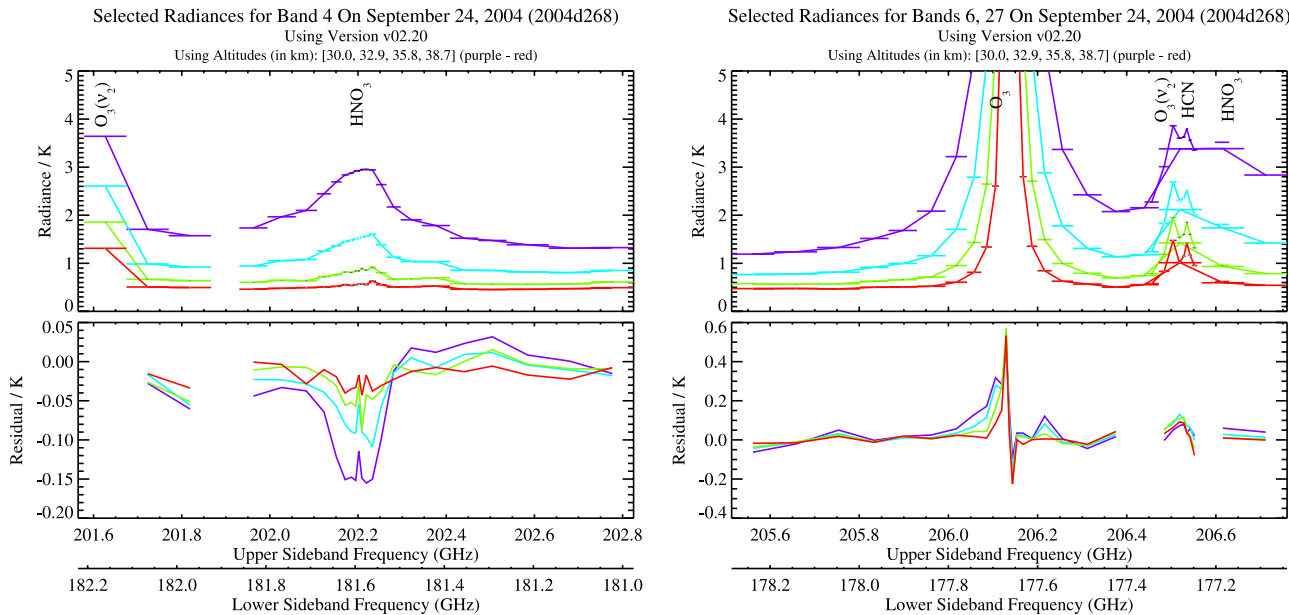


Figure 2. Sample radiances and residuals from the Aura MLS 190-GHz radiometer for (left) band 4 and (right) bands 6 and 27. (top) Global average radiances for a representative day (24 September 2004), expressed as brightness temperature (in K), for four selected tangent point altitudes from 30.0 km (purple) to 38.7 km (red). The MLS signal is a combination of incoming radiance above (upper sideband, upper x axis) and below (lower sideband, lower x axis) the 191.900 GHz local oscillator. The widths of the various MLS spectral channels are denoted by the horizontal bars. (bottom) Average residual of the fit achieved by the MLS version 2.2 retrieval algorithms. Residuals for channels not used in the retrievals are not shown.

vative value that potentially discards a significant fraction of “good” data points while not necessarily identifying all “bad” ones.

[11] Additional information on the success of the retrieval is conveyed by the “Convergence” field, which compares the fit achieved for each “chunk” of ~ 10 profiles to that expected by the retrieval algorithms; values around 1.0 typically indicate good convergence. Many, but not all, profiles with larger (i.e., poorer) values of “Convergence” are filtered out by the other quality control measures; for completeness, we recommend rejecting profiles for which “Convergence” exceeds 1.8. On a typical day this threshold for “Convergence” discards a negligible fraction of data, but on occasion it leads to the elimination of more than 1% of the HNO₃ profiles.

[12] Finally, we note that the MLS data processing algorithms sometimes produce negative mixing ratios, especially for noisy retrievals such as HNO₃ when values are very low. Though unphysical, the negative mixing ratios must be retained in any scientific studies making use of averages of data, in order to avoid introducing positive biases into the MLS averages.

2.3. Signature of HNO₃ in the MLS Radiances

[13] Sample radiances for a representative day of Aura MLS observations are shown in Figures 1 and 2. More specifics about the MLS spectrometers, the spectral bands they cover, and their target molecules are given by *Waters et al.* [2006], and a full representation of the MLS spectral coverage superimposed on a calculated atmospheric spec-

trum is presented by *Read et al.* [2006]. Figure 1 illustrates radiances in the 240-GHz region of the spectrum, from which the MLS HNO₃ measurements at and below (i.e., at pressures equal to or larger than) 10 hPa are retrieved. To provide context several bands are shown; the strong spectral features evident in Figure 1 (top) are all due to emission from O₃ lines, with the exception of the feature at ~ 234 GHz in the lower sideband (lower x axis), which is due to O¹⁸O emission. Information on HNO₃ in the upper troposphere and lower stratosphere is derived from the differences of channels two (~ 244.2 GHz, upper sideband, upper x axis) and four (~ 231.7 GHz, lower sideband) relative to channel three (~ 246.8 GHz, upper sideband) of the band 33 wideband filter; these differences have a typical amplitude of ~ 20 K in the lower stratosphere. The residuals shown in Figure 1 (bottom) indicate that on average the retrievals are fitting the radiances to within $\sim 2\text{--}3\%$ (~ 0.5 K) for these channels.

[14] Figure 2 shows two different portions of the 190-GHz region of the spectrum, both of which contribute to the HNO₃ retrievals above (i.e., at pressures less than) 10 hPa. The spectral feature in Figure 2 (left) (band 4) arises from a cluster of HNO₃ lines near 181.6 GHz in the lower sideband. The main feature in Figure 2 (right) (bands 6 and 27) is from a strong O₃ line at 206.1 GHz in the upper sideband; the secondary peak is associated with an O₃(ν_2) line at 206.5 GHz and an HCN line near 177.3 GHz in the lower sideband. The signal from a cluster of nearby HNO₃ lines is visible in the wing of the ozone line around

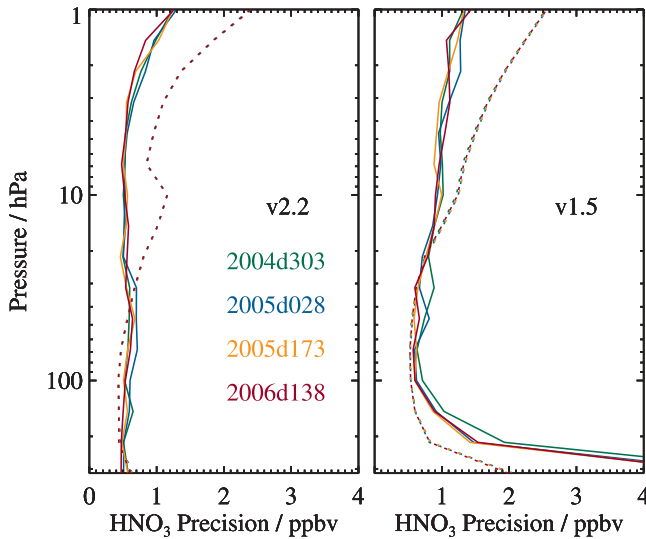


Figure 3. Precision of the (left) v2.2 and (right) v1.5 MLS HNO₃ measurements for four representative days (see legend). Solid lines depict the observed scatter in the 20°-wide latitude band centered around the equator; for each of the days pictured here, ~350–375 profiles fall in this latitude bin. Dotted lines depict the theoretical precision estimated by the retrieval algorithm.

206.7 GHz. For these bands the radiances are being fit to within $\sim 5\%$.

2.4. Precision, Spatial Resolution, and Vertical Range

[15] The precision of the MLS HNO₃ measurements is estimated empirically by computing the standard deviation of the profiles in a narrow equatorial band where natural atmospheric variability should be small relative to the measurement noise. Because meteorological variation is never completely negligible, however, this procedure produces an upper limit on the precision. As shown in Figure 3, the observed scatter in the v2.2 data is ~ 0.6 –0.7 ppbv throughout the range from 215 to 3.2 hPa, above which it increases sharply. The scatter is essentially invariant with time, as seen by comparing the results for the different days shown in Figure 3. Because HNO₃ exhibits little diurnal variation, we also estimate precision by calculating the standard deviation of the differences between matched measurement points from the ascending (day) and descending (night) sides of the orbit within the 50°S–50°N latitude band. Precision estimates based on this approach (not shown) are very similar. Furthermore, no significant offsets between HNO₃ values measured on the crossing orbits are found.

[16] The single-profile precision estimates cited here are, to first order, independent of latitude and season, but it should be borne in mind that the scientific utility of individual MLS profiles (i.e., signal to noise) varies with HNO₃ abundance. At some latitudes and altitudes and in some seasons, the single-profile precision exceeds typical HNO₃ mixing ratios, necessitating the use of averages for scientific studies. In most cases, precision can be improved by averaging, with the precision of an average of N profiles

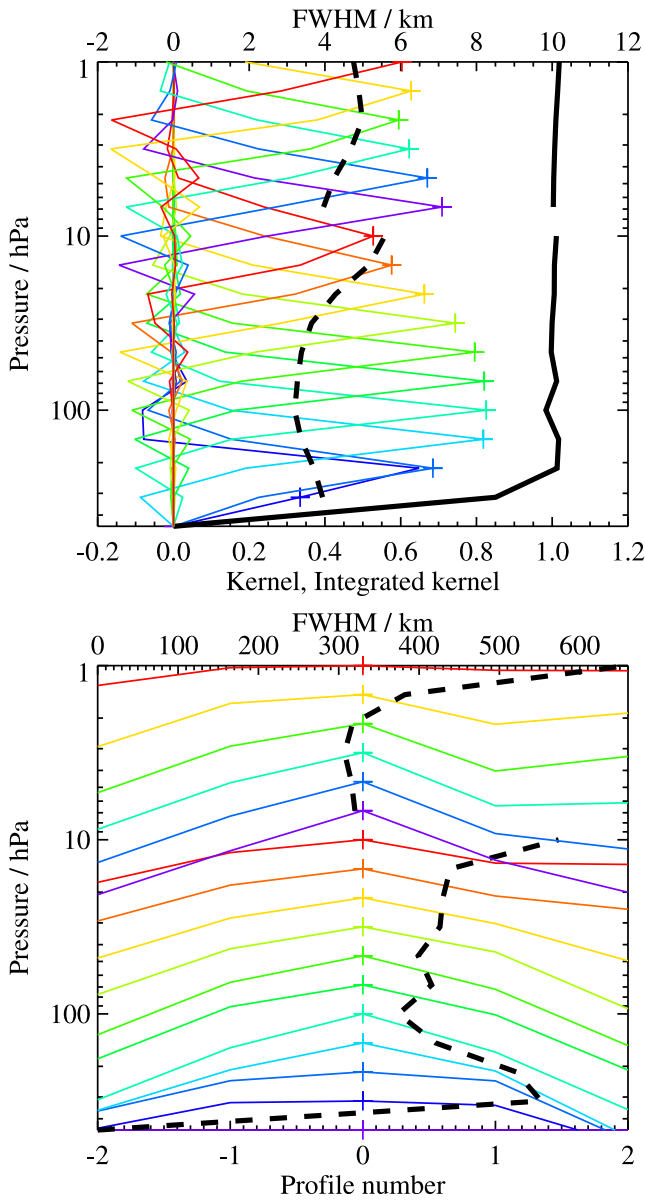
being $1/\sqrt{N}$ times the precision of an individual profile (note that this is not the case for averages of successive along-track profiles, which are not completely independent because of horizontal smearing).

[17] The observational determination of the precision is compared in Figure 3 to the theoretical precision values reported by the Level 2 data processing algorithms. Although the two estimates compare very well in the lower portion of the profile, above 22 hPa the predicted precision substantially exceeds the observed scatter. This indicates that the a priori information and the vertical smoothing applied to stabilize the retrieval are influencing the results at the higher retrieval levels. In addition, the “notch” in the theoretical precision profile at 10 hPa arises from switching from the 240-GHz to the 190-GHz retrievals in composing the standard HNO₃ product. Because the theoretical precisions take into account occasional variations in instrument performance, the best estimate of the precision of an individual data point is the value quoted for that point in the L2GP files, but it should be borne in mind that this approach overestimates the actual measurement noise at pressures less than 22 hPa.

[18] For comparison, Figure 3 also shows precision estimates for the v1.5 MLS HNO₃ data. The HNO₃ data in v2.2 have been greatly improved over those in v1.5, with much less observed scatter, especially at the lowest retrieval levels. Several factors account for the improvements in v2.2. First, approximations in the forward model are more accurate for HNO₃ in v2.2 than in v1.5. In both versions, the spectral grid for evaluating radiances in each channel is optimized for O₃, ¹⁸O₂, and CO for the 240-GHz radiometer. In v1.5 this leads to spectral integration errors in the vicinity of HNO₃ lines, particularly at low pressures. V2.2 utilizes a prefrequency averaging (PFA) approximation, whereby HNO₃ absorption is accurately convolved with the channel’s spectral response offline and stored in tables for subsequent use in radiative transfer calculations. The PFA approximation is highly accurate for weak lines (such as HNO₃) in the presence of strong O₃ lines. Second, unexplained radiances are accounted for in v1.5 through retrieval of a spectrally flat additive “baseline” term for each scan height, whereas in v2.2 a spectrally flat “extinction” parameter is retrieved for each retrieval level. This approach provides a better physical model for uncertainties in knowledge of middle tropospheric H₂O, cloud contamination, and the dry continuum than an additive baseline [e.g., Livesey *et al.*, 2006]. Third, the vertical regularization (smoothing) has been increased for HNO₃ in v2.2, especially at the lowest retrieval levels. As shown in the systematic error analysis in section 2.5, the uncertainty in the HNO₃ data increases sharply at pressures larger than 100 hPa, as a result of declining HNO₃ concentrations and a weaker, broader HNO₃ line in the spectrum. Increasing the smoothing makes the profile less prone to erratic behavior caused by systematic errors but incurs the penalty of poorer resolution, as discussed below. In v2.2 the retrieval has been “tuned” to mitigate oscillations at the expense of some loss of vertical resolution information. The consequences of these changes are discussed further in section 2.6.

[19] As mentioned previously, the MLS retrieval algorithms employ a two-dimensional approach that accounts for the fact that the radiances for each limb scan are

influenced by the state of the atmosphere at adjacent scans along the forward looking instrument line of sight [Livesey *et al.*, 2006]. The resolution of the retrieved data can be described using “averaging kernels” [e.g., Rodgers, 2000]; the two-dimensional nature of the MLS data processing system means that the kernels describe both vertical and horizontal resolution. Smoothing, imposed on the retrieval system in both the vertical and horizontal directions to enhance retrieval stability and precision, reduces the inherent resolution of the measurements. Consequently, the vertical resolution of the v2.2 HNO₃ data, as determined from the full width at half maximum of the rows of the averaging kernel matrix shown in Figure 4, is 3–4 km in the upper troposphere and lower stratosphere, degrading to ~5 km in the middle and upper stratosphere. Note that the averaging kernels for the 215 and 316 hPa retrieval surfaces overlap nearly completely, indicating that the 316 hPa retrieval provides essentially no independent information. Figure 4 also shows horizontal averaging kernels, from



which the along-track horizontal resolution is determined to be 400–500 km over most of the vertical range, improving to ~300 km in the upper stratosphere. The cross-track resolution, set by the widths of the fields of view of the 190-GHz and 240-GHz radiometers, is ~10 km.

[20] Although HNO₃ is retrieved (and reported in the L2GP files) over the range from 316 to 0.001 hPa, on the basis of the drop off in precision and resolution and the lack of independent information contributed by the measurements, the data are not deemed reliable at the extremes of the retrieval range. The HNO₃ behavior at 316 hPa is consistent with the findings of Livesey *et al.* [2007b], who concluded that the poor quality of the MLS O₃ observations at 316 hPa reflects an inability of the MLS retrievals to correctly interpret the radiances measured at tangent pressures from ~250–316 hPa. Because the MLS radiances in the upper troposphere in the 240-GHz region are dominated by emission from O₃ lines (as shown in Figure 1), the failure of the O₃ retrieval at 316 hPa suggests that the HNO₃ data at that level are also unlikely to be useful. Thus we recommend that v2.2 HNO₃ be used for scientific studies only at the levels between 215 and 3.2 hPa.

2.5. Quantification of Systematic Uncertainty

[21] A major component of the validation of MLS data is the quantification of the various sources of systematic uncertainty. Systematic uncertainties arise from instrumental issues (e.g., radiometric calibration, field of view characterization), spectroscopic uncertainty, and approximations in the retrieval formulation and implementation. This section summarizes the relevant results of a comprehensive quantification of these uncertainties that was performed for all MLS products. More information on this assessment is given by Read *et al.* [2007, Appendix A].

Figure 4. Typical two-dimensional (vertical and horizontal along-track) averaging kernels for the MLS v2.2 HNO₃ data at the equator; variation in the averaging kernels is sufficiently small that these are representative for all profiles. Colored lines show the averaging kernels as a function of MLS retrieval level, indicating the region of the atmosphere from which information is contributing to the measurements on the individual retrieval surfaces, which are denoted by plus signs in corresponding colors. The dashed black line indicates the resolution, determined from the full width at half maximum (FWHM) of the averaging kernels, approximately scaled into kilometers (top axis). The discontinuity reflects the transition between the 240-GHz retrievals (used at and below 10 hPa) and the 190-GHz retrievals (used above 10 hPa). (top) Vertical averaging kernels (integrated in the horizontal dimension for five along-track profiles) and resolution. The solid black line shows the integrated area under each kernel (horizontally and vertically); values near unity imply that the majority of information for that MLS data point has come from the measurements, whereas lower values imply substantial contributions from a priori information. (bottom) Horizontal averaging kernels (integrated in the vertical dimension) and resolution. The individual horizontal averaging kernels are scaled in the vertical direction such that a unit change is equivalent to one decade in pressure.

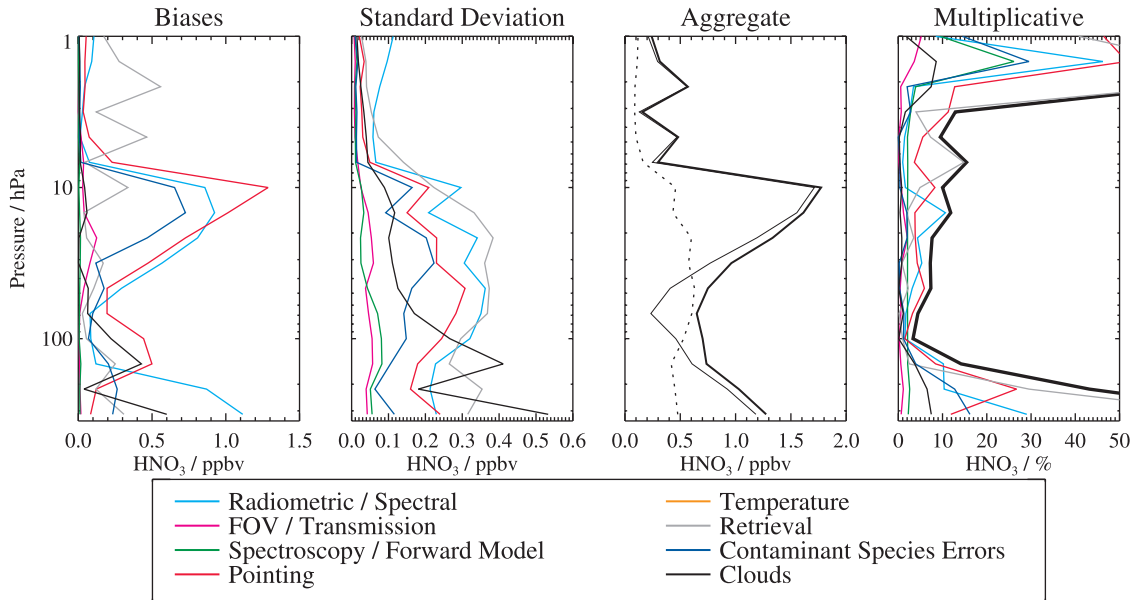


Figure 5. Estimated impact (2σ) of various families of systematic uncertainty on the MLS HNO₃ observations. The first two panels show the possible biases (first panel) and standard deviation (second panel) of the additional scatter introduced by the various families of uncertainty, with each family denoted by a different colored line. Cyan lines denote uncertainties in MLS radiometric and spectral calibration. Magenta lines show uncertainties associated with the MLS field of view and antenna transmission efficiency. Red lines depict errors associated with MLS pointing uncertainty. The impacts of uncertainties in spectroscopic databases and forward model approximations are denoted by the green line, while those associated with retrieval formulation are shown in grey. The gold lines indicate uncertainty resulting from errors in the MLS temperature product, while the blue lines show the impact of similar “knock on” errors in other species. Finally, the typical impact of cloud contamination is denoted by the black line. The third panel shows the root sum square (RSS) of all the possible biases (thin solid line), all the additional scatter (thin dotted line), and the RSS sum of the two (thick solid line). The fourth panel shows the scaling uncertainty introduced by the various families of errors, with the thick black line showing the RSS of all the reported scaling uncertainties.

[22] The impact on MLS measurements of radiance (or pointing where appropriate) of each identified source of systematic uncertainty has been quantified and modeled. These modeled impacts correspond to either 2σ estimates of uncertainties in the relevant parameters, or an estimate of their maximum reasonable errors based on instrument knowledge and/or design requirements. The effect of these perturbations on retrieved MLS products has been quantified for each source of uncertainty by one of two methods.

[23] In the first method, sets of modeled errors corresponding to the possible magnitude of each uncertainty have been applied to simulated MLS cloud-free radiances, based on a model atmosphere, for a whole day of MLS observations. These sets of perturbed radiances have then been run through the routine MLS data processing algorithms, and the differences between these runs and the results of the “unperturbed” run have been used to quantify the systematic uncertainty in each case. The impact of the perturbations varies from product to product and among uncertainty sources. Although the term “systematic uncertainty” is often associated with consistent additive and/or multiplicative biases, many sources of “systematic” uncertainty in the MLS measurement system give rise to additional scatter in the products. For example, although an error in the O₃ spectroscopy is a bias on the fundamental

parameter, it has an effect on the retrievals of species with weaker signals (e.g., HNO₃) that is dependent on the amount and morphology of atmospheric ozone. The extent to which such terms can be expected to average down is estimated to first order by these “full up studies” through their separate consideration of the bias and scatter each source of uncertainty introduces into the data. The difference between the retrieved product in the unperturbed run and the original “truth” model atmosphere is taken as a measure of uncertainties due to retrieval formulation and numerics. To test the sensitivity of the retrieved mixing ratios to the a priori information, another retrieval of the unperturbed radiances is performed with the a priori adjusted by a factor of 1.5.

[24] In the second method, the potential impact of some remaining (typically small) systematic uncertainties has been quantified through calculations based on simplified models of the MLS measurement system [see Read *et al.*, 2007]. Unlike the “full up studies,” these calculations only provide estimates of “gain uncertainty” (i.e., possible multiplicative error) introduced by the source in question; this approach does not quantify possible biases or additional scatter for these minor sources of uncertainty.

[25] Figure 5 summarizes the results of the uncertainty characterization for the MLS v2.2 HNO₃ measurements.

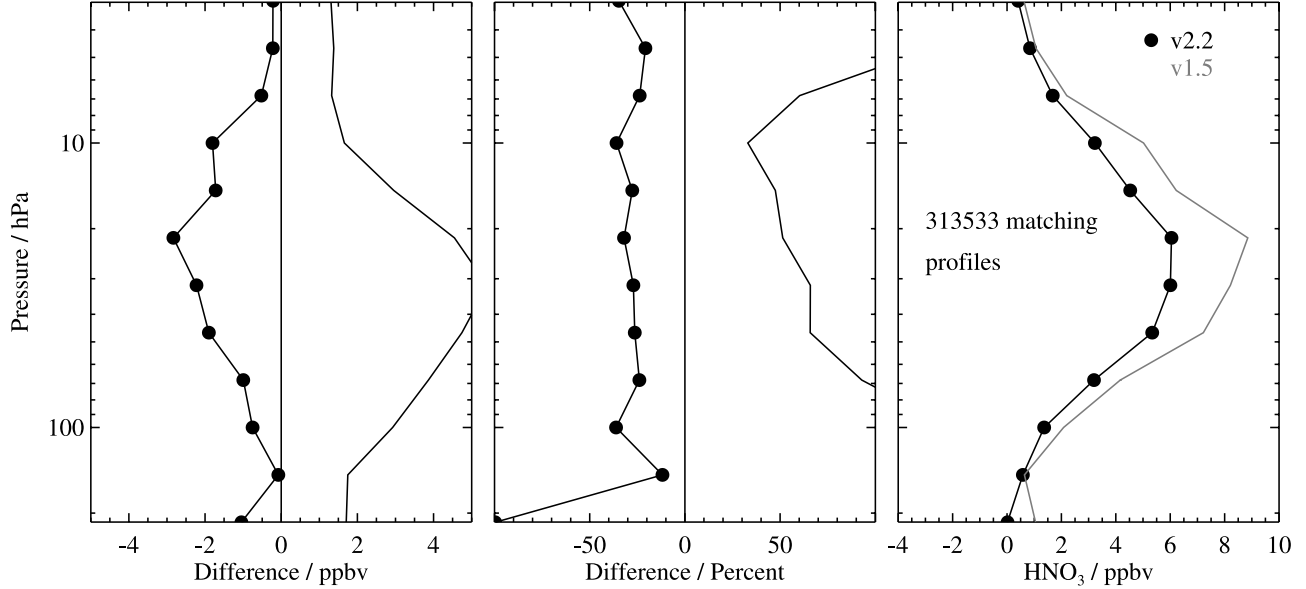


Figure 6. Comparison of v2.2 and v1.5 Aura MLS HNO₃ measurements from 93 d for which both versions of data were available at the time of writing (February 2007). (left) Absolute differences (v2.2–v1.5). The black line with dots (symbols indicate MLS retrieval surfaces) shows mean differences, and the solid black line shows the standard deviation of the differences. (middle) Same, for percent differences (computed relative to v1.5). (right) Global mean profiles for v2.2 (black, with dots) and v1.5 (grey).

The colored lines show the magnitudes of expected biases, additional scatter, and possible scaling errors the various sources of uncertainty may introduce into the data, and should be interpreted as 2- σ estimates of their probable magnitude. The largest potential error source throughout much of the profile is uncertainty in the field of view pointing offsets between various bands of the 240-GHz radiometer (red lines); this uncertainty results in biases of as much as ± 1.3 ppbv at 10 hPa, scatter of ± 0.2 – 0.3 ppbv over much of the profile, and a scaling error as large as $\pm 25\%$ at 215 hPa. (Note that the pointing uncertainty for the MLS 190-GHz HNO₃ product, though substantially smaller, also peaks at 10 hPa.) Another dominant source of uncertainty originates from the spectral signature induced in the calibrated MLS radiances by departures from a linear response within the signal chains leading to gain compression (cyan lines); this can lead to biases as large as ± 1 ppbv at 15 and 215 hPa, scatter of ± 0.2 – 0.4 ppbv over a broad vertical range, and a scaling error of $\pm 10\%$ at 15 and 147–215 hPa. Contamination from possible errors in O₃ (retrieved in the same phase as HNO₃ [Livesey et al., 2006]) arising from errors in the O₃ line shape (blue lines) causes biases of more than ± 0.5 ppbv from 22 to 10 hPa, scatter of ± 0.1 – 0.2 ppbv in most of the stratosphere, and multiplicative error of $\pm 12\%$ at 215 hPa. Retrieval numerics (grey lines) are a major source of scatter (± 0.3 – 0.4 ppbv) throughout the vertical range; although these simulation results also suggest a scaling uncertainty of $\pm 30\%$ at 215 hPa, a reliable estimate is hampered by the (albeit geophysically appropriate) lack of dynamic range in the “truth” mixing ratios used for this level, and the actual scaling uncertainty contributed by retrieval numerics is likely to be much smaller (e.g., less than $\pm 5\%$ as at 147 hPa).

[26] Finally, although the MLS observations are unaffected by thin cirrus clouds or stratospheric aerosols, thick

clouds associated with deep convection can have an impact on the MLS radiances. The MLS Level 2 data processing algorithms discard or downplay radiances identified (through comparison with predictions from a clear-sky model) as being strongly affected by clouds [Livesey et al., 2006]. The contribution of cloud effects to the systematic uncertainty, both from the presence of clouds not thick enough to be screened out by the cloud filtering and from the loss of information through omission of cloud-impacted radiances, has been quantified by adding scattering from a representative cloud field to the simulated radiances and comparing retrievals based on these radiances to the unperturbed results. The cloud-induced effects shown in Figure 5 are estimated by considering only the cloudy profiles (as defined by the known amount of cloud in the “truth” field). This analysis indicates that the presence of thick clouds (black lines) can potentially induce in the measurements biases as large as ± 0.5 ppbv at 147 hPa, scatter of ± 0.2 – 0.4 ppbv from 68 to 215 hPa, and a multiplicative error exceeding $\pm 5\%$ at 215 hPa.

[27] Other potential sources of uncertainty are found to contribute negligibly (less than ~ 0.1 ppbv bias or scatter, less than 2% scaling error). In aggregate, systematic uncertainties are estimated to induce in the v2.2 HNO₃ measurements biases that vary with altitude between ± 0.5 and ± 2 ppbv and multiplicative errors of ± 5 – 15% throughout the stratosphere, rising to $\sim \pm 30\%$ at 215 hPa. The scatter introduced into the data by the various sources of uncertainty is estimated to be $\sim \pm 0.6$ ppbv throughout most of the vertical domain, in very good agreement with the empirical determination of the precision discussed in section 2.4.

2.6. Comparison With v1.5 HNO₃ Data

[28] Early validation analyses [Froidevaux et al., 2006; Barret et al., 2006] revealed that the v1.5 Aura MLS HNO₃

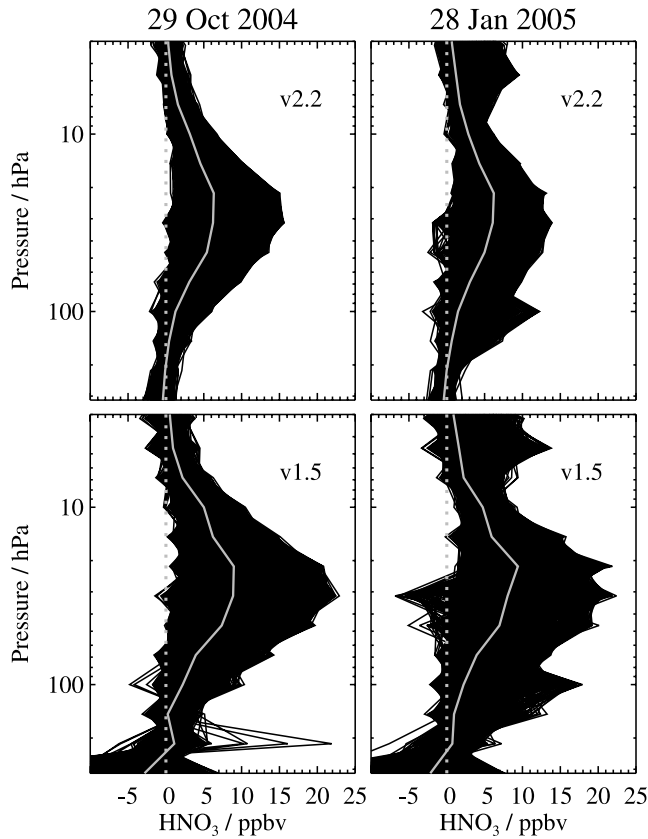


Figure 7. Vertical profiles of (top) v2.2 and (bottom) v1.5 Aura MLS HNO₃ for two selected days (29 October 2004 and 28 January 2005), chosen to represent a range of atmospheric conditions. All ~ 3450 profiles passing the quality control screening each day are shown (black lines), with the global mean profile overlaid (grey solid line).

data were biased high by $\sim 10\text{--}40\%$ relative to nearly coincident satellite and balloon-borne measurements. The cause of this artifact was traced to a typographical error in one of the spectroscopy files used in the v1.5 processing. Specifically, the ground-state rotational partition function was inadvertently used in place of the vibrational-rotational partition function. The spectroscopy file tabulates the line strengths at 300 K and the partition functions at 300, 225, and 150 K. Determination of line strengths at temperatures other than 300 K requires accurate calculation of the ratio of the partition function at 300 K to that at the desired temperature, which is derived from the table in the file. Using the ground-state partition function instead of the ro-vibrational partition function caused an underestimation of the line strengths at typical stratospheric temperatures. This error has been rectified in v2.2. Figure 6 shows the comparison between v1.5 and v2.2 for 93 d for which both versions of data were available at the time of writing (February 2007). Mean differences reach 3 ppbv at the profile peak, with v2.2 HNO₃ mixing ratios $\sim 25\text{--}35\%$ lower than the corresponding v1.5 values throughout the vertical range from 100 to 3 hPa.

[29] In addition to overall smaller mixing ratios and, as discussed in section 2.4, better precision, the v2.2 HNO₃ retrievals have been improved in other ways. Comparison of individual measurements in Figure 7 shows that, although

still somewhat oscillatory in the vertical, the v2.2 profiles exhibit fewer large excursions and generally have smoother global mean profiles than in v1.5. Most notably, the unrealistic behavior at the lowest retrieval levels (at pressures greater than 68 hPa), pervasive enough to significantly affect zonal mean values in v1.5, has been substantially reduced (Figure 8). As described in section 2.4, several refinements, such as more accurate approximations for HNO₃ in the forward model, changes to the retrieval approach, and increased vertical smoothing, all contributed to significant improvements in the v2.2 HNO₃ data, including mitigation of oscillations.

[30] Amelioration of the strong oscillations in the retrieved profiles has enhanced the scientific utility of the v2.2 data, especially in the upper troposphere/lower stratosphere, but also generally throughout the vertical domain. This is illustrated by two aspects of the profiles for 28 January 2005 (Figures 7 and 8) that stand out more distinctly in v2.2 than in v1.5. A secondary peak in the HNO₃ at 4.6 hPa is most likely a real atmospheric feature reflecting HNO₃ enhancement in response to solar storm activity [e.g., Orsolini *et al.*, 2005], and another secondary maximum at 100 hPa may represent the signature of renitification from evaporation of polar stratospheric cloud particles sedimenting from above, as seen in aircraft measurements made in the lowermost stratosphere at this time [Kleinböhl *et al.*, 2005; Dibb *et al.*, 2006].

3. Comparison With UARS MLS Climatology

[31] The MLS onboard UARS measured the global distribution of stratospheric HNO₃ for much of the 1990s, albeit with approximately monthly gaps in high-latitude coverage arising from UARS yaw maneuvers and with significantly reduced temporal sampling in the latter half of the decade. A comprehensive overview of the seasonal, interannual, and interhemispheric variations in HNO₃ throughout the lower and middle stratosphere (420–960 K potential temperature) was produced from the UARS MLS data by Santee *et al.* [2004]. In that study, averages were

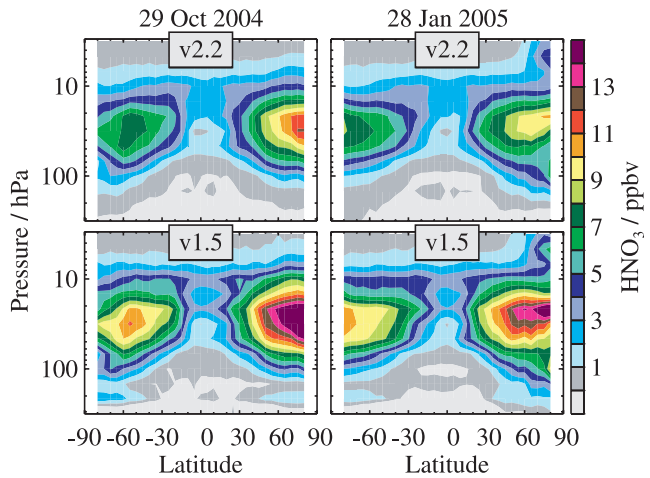


Figure 8. Zonal mean cross sections of (top) v2.2 and (bottom) v1.5 Aura MLS HNO₃ for the same days as shown in Figure 7.

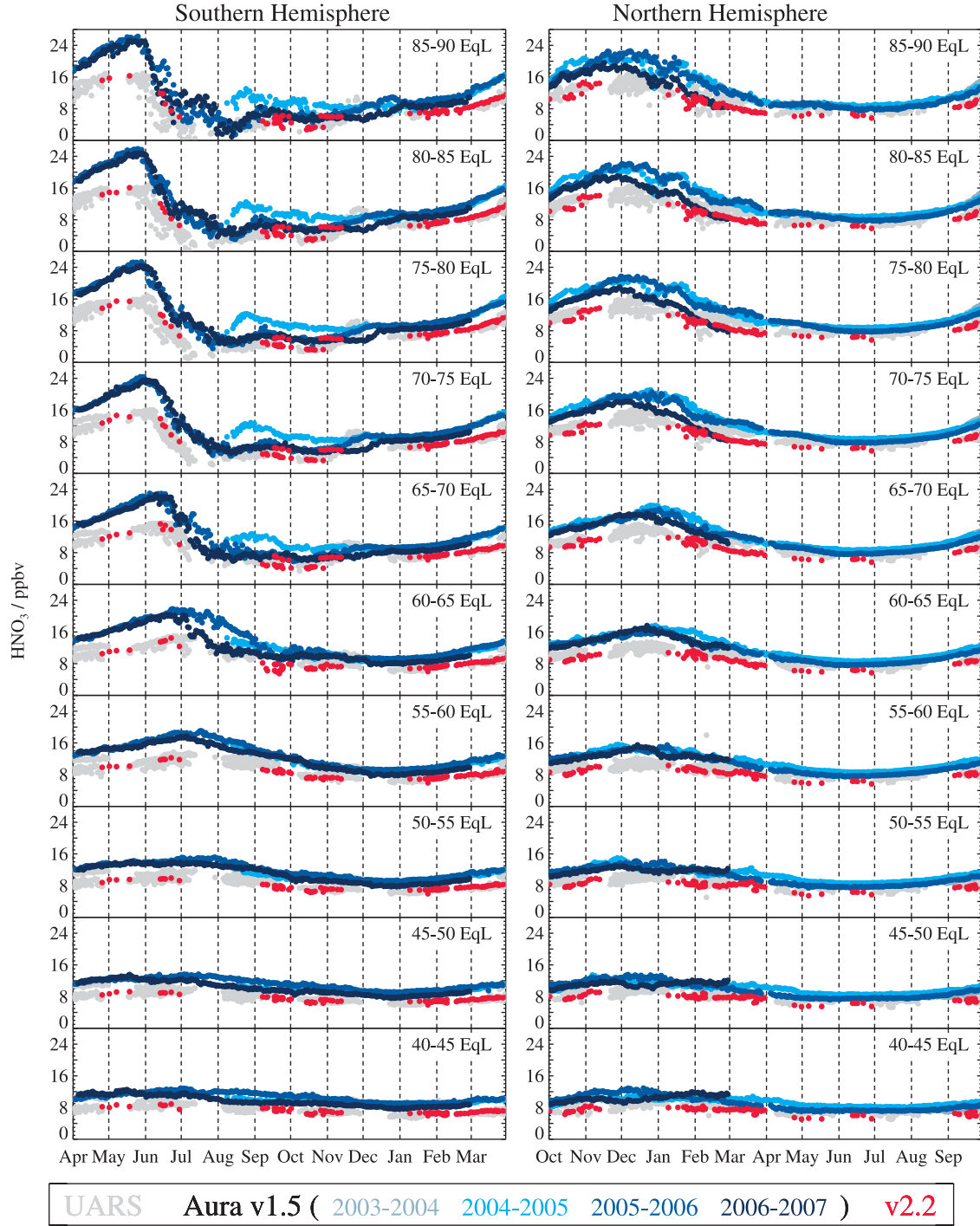


Figure 9. Time series of MLS HNO₃ measurements at 580 K potential temperature (corresponding to ~ 32 hPa, 22 km) for the (left) Southern and (right) Northern Hemispheres. Daily means were calculated by binning the measurements into 5° equivalent latitude (EqL) bands and averaging. Grey dots depict version 6 UARS MLS HNO₃ data taken over the period 1991–2000; blue dots depict version 1.5 (v1.5) Aura MLS HNO₃ data, with different shades of blue representing different years as indicated in the legend, and red dots depict version 2.2 (v2.2) Aura MLS data. Dashed vertical lines demarcate calendar months.

calculated over equivalent latitude (EqL), the latitude encircling the same area as a given contour of potential vorticity (PV) [Butchart and Remsberg, 1986]; using EqL rather than geographic latitude provides a vortex-centered view, ensur-

ing that only similar air masses are averaged together and preserving strong gradients across the vortex edge.

[32] Taking a similar approach with Aura MLS measurements provides a means of quantitatively comparing to the HNO₃ climatology derived from UARS MLS data. The

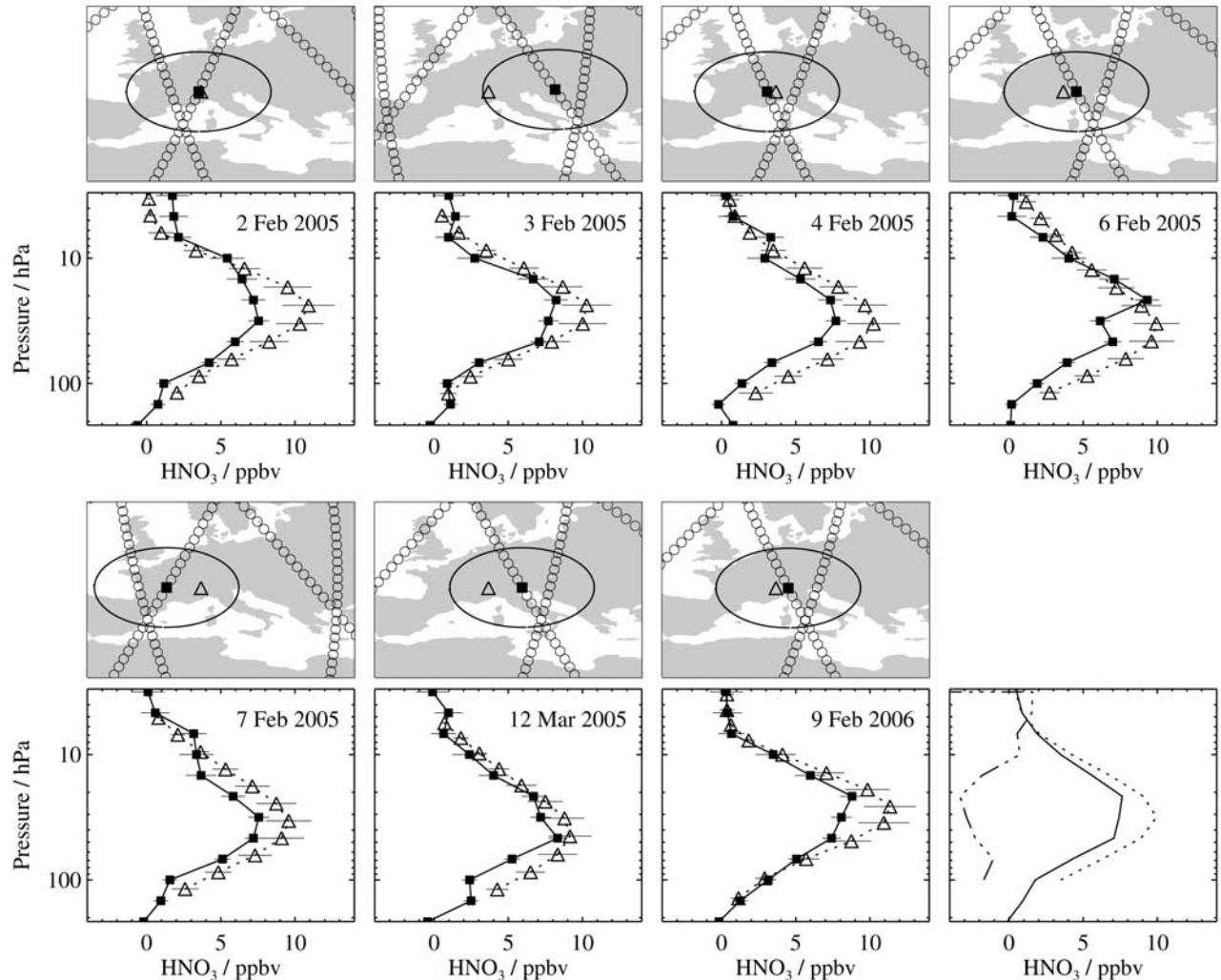


Figure 10. The first through seventh panels show a comparison of the closest (geographically and temporally) available MLS v2.2 HNO₃ profile to the GBMS measurements from 7 d in February/March 2005 and February 2006. The top plots of each panel show MLS measurement tracks (open circles) in the vicinity of the Testa Grigia site of the GBMS instrument (open triangle). The MLS data point closest to the GBMS measurement is indicated by the solid square; the 800-km radius around the closest MLS point is overlaid. The bottom plots of each panel show profiles of HNO₃ from MLS (solid squares) and GBMS (open triangles), corresponding to the symbols in the top plots. For MLS the error bars represent the estimated precision of the HNO₃ data reported by the retrieval system; for GBMS the error bars represent the overall uncertainty in the data (see text). The eighth panel shows mean HNO₃ profiles from MLS (solid line) and GBMS (dotted line), and mean differences (MLS-GBMS) computed from the differences on the individual days (dash-dot line).

daily means in Figure 9 were computed by binning both the UARS and the Aura MLS HNO₃ measurements into 5° EqL bands and averaging; results are shown for 10 EqL bands over annual cycles in both hemispheres. All UARS MLS data collected from 1991 through 2000 are represented by grey dots. To illustrate the degree of interannual variability in the Aura MLS data record, the v1.5 HNO₃ measurements obtained in each year since launch in July 2004 are depicted in different shades of blue, with results from the v2.2 retrievals performed to date overlaid in red. Data from both MLS instruments have been interpolated to the 580 K potential temperature surface (~32 hPa, 22 km) near the peak in the HNO₃ vertical profile, using temperatures from

the U.K. Met Office analyses [Swinbank *et al.*, 2002] for UARS MLS and from NASA's Global Modeling and Assimilation Office Goddard Earth Observing System Version 4.0.3 (GEOS-4) [Bloom *et al.*, 2005] for Aura MLS.

[33] Both the latitudinal variation of HNO₃ and its evolution over an annual cycle match those in the climatology based on the multiyear UARS MLS data set. Figure 9, however, clearly shows the pervasive high bias in the v1.5 Aura MLS HNO₃ measurements. Correction of the spectroscopy error has eliminated this high bias in v2.2, whose values agree with or are slightly lower than climatological ones in all EqL bands in all seasons. (Note that the spectroscopy error in the v1.5 Aura MLS HNO₃ measure-

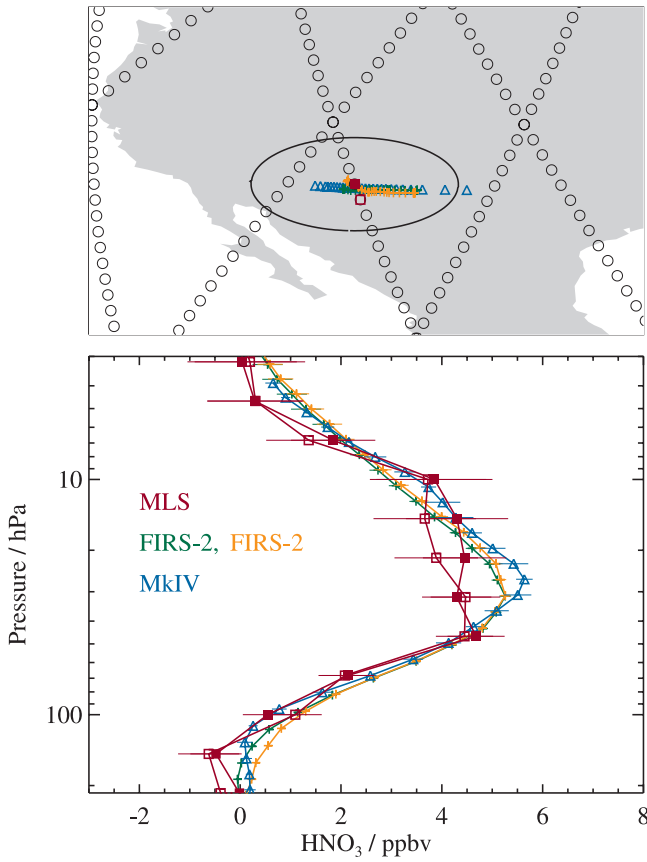


Figure 11. (top) Path traversed by measurements from the balloon-borne MkIV (blue triangles) and FIRS-2 (green and orange crosses represent two separate profiles) instruments during the flight from Fort Sumner, NM, on 23–24 September 2004. Measurement tracks from nearby MLS orbits are also shown (open circles). The two MLS data points closest to the balloon measurements (geographically and temporally) are indicated by red squares, with the closer one denoted by a solid symbol; the 500-km radius around the closest MLS point is overlaid in black. (bottom) Profiles of HNO₃ from MLS (red squares), MkIV (blue triangles), and FIRS-2 (green and orange crosses), corresponding to the symbols in the top image. Error bars represent the estimated precisions of each instrument, taken from the data files.

ments did not affect the HNO₃ measurements from UARS MLS.) Similar results are obtained at other levels throughout the stratosphere (not shown).

4. Comparisons With Other Observations

[34] In this section the accuracy of the Aura MLS v2.2 HNO₃ measurements is assessed through comparisons with correlative data from a variety of different platforms, some of which were acquired in dedicated Aura validation campaigns. For these comparisons we use the traditional approach of considering matched pairs of profiles that are closely colocated both geographically and temporally. The coincidence criteria used to select the matches vary and are stated in each subsection below. In some cases, use of an

additional filter based on the potential vorticity of the profiles (to ensure that only meteorologically consistent air masses are compared) was explored but was found to have little impact on the average differences. The vertical resolution of most of the correlative HNO₃ measurements used here is not greatly different from that of MLS. Therefore, although strictly speaking the higher-resolution measurements should be smoothed by applying the averaging kernels of the lower-resolution data, in practice it has little effect on these comparisons; for those cases in which differences are computed, the correlative profiles have been linearly interpolated in log pressure to the fixed MLS retrieval pressure surfaces.

4.1. Ground-Based Measurements

[35] The Ground-Based Millimeter-wave Spectrometer (GBMS) has been operated at a variety of sites to obtain profiles of several different stratospheric constituents; in particular, HNO₃ is measured using a compact cluster of emission lines centered at 269.24 GHz. Details of the GBMS experimental apparatus and retrieval technique are given by *de Zafra et al.* [1997], *Muscare et al.* [2002], and references therein. The deconvolution code for retrieving HNO₃ from the GBMS spectra currently employs spectroscopic data from the Jet Propulsion Laboratory (JPL)

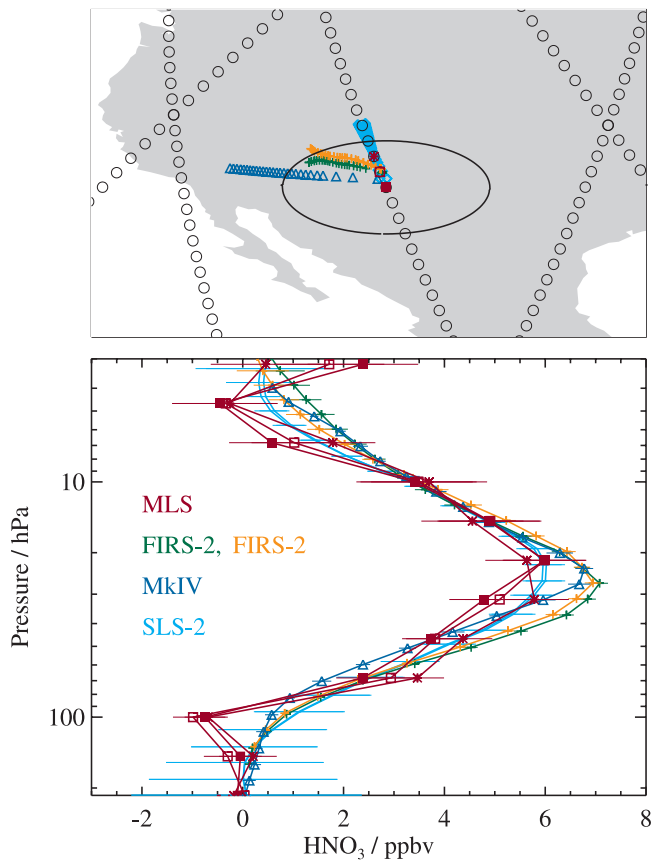


Figure 12. As in Figure 11, for the flight from Fort Sumner, NM, on 20–21 September 2005, except that the three closest MLS profiles are shown and two profiles from a third balloon-borne instrument, SLS-2, are added (cyan diamonds on map, lines in plot of profiles).

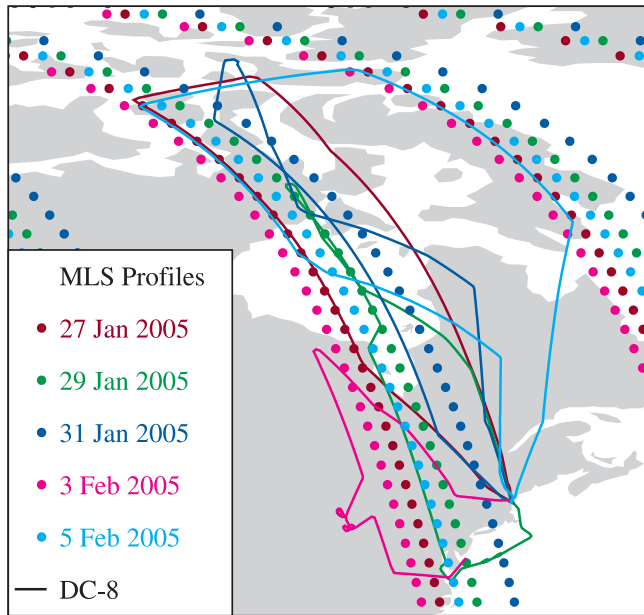


Figure 13. Flight tracks (lines color-coded by date) of the NASA DC-8 aircraft during the Polar Aura Validation Experiment (PAVE) mission conducted from Portsmouth, New Hampshire, in January/February 2005. Only flights on days for which both MLS v2.2 and SAGA data are available are shown. The MLS ground tracks on these days are indicated by solid dots in corresponding colors.

database (current data available at <http://spec.jpl.nasa.gov>) [Pickett et al., 1998] and pressure broadening coefficients from Goyette et al. [1988], the same sources of spectroscopic parameters as used by MLS. HNO₃ is measured over an altitude range of ~15–40 km; vertical resolution is ~5–8 km, although the retrievals typically locate the altitude of the profile peak to within ~2 km in the middle and lower stratosphere [de Zafra et al., 1997]. As stratospheric air moves above the site, GBMS samples an air mass 200–300 km in length during the ~3 h of integration time for each measurement [Muscati et al., 2002]. The overall 1- σ uncertainty in the retrieved mixing ratios (including both systematic and random errors) varies with altitude and time but is typically 16–22% or 0.5 ppbv, whichever is larger [de Zafra et al., 1997; Muscati et al., 2002].

[36] Here we compare MLS HNO₃ measurements with those from GBMS made at Testa Grigia, a site in the Alps on the border between Italy and Switzerland (45.9°N, 7.7°E). Figure 10 shows the closest MLS profile to the GBMS measurements for 7 d in February/March 2005 and February 2006 for which v2.2 MLS data were available at the time of writing (coincidence criteria: ±1° in latitude, ±12° in longitude, ±24 h). The overall shapes of the profiles are very similar. Smaller-scale vertical structure evident in MLS but not GBMS data (e.g., the notch in the profile on 6 February 2005) may represent real atmospheric features not discernible in the coarser-resolution ground-based measurements. Day-to-day variations in the HNO₃ profile observed by GBMS are tracked well by MLS, but the MLS HNO₃ values are systematically low relative to those

measured by GBMS, with differences as large as ~3 ppbv (20–30%) on average near the profile peak.

4.2. Balloon Measurements

[37] As part of the Aura validation effort, measurements of HNO₃ were obtained near Aura overpasses from several remote sounding instruments during balloon campaigns carried out from Fort Sumner, New Mexico, in September of 2004 and 2005. One such instrument is the JPL MkIV solar occultation Fourier Transform Infrared (FTIR) spectrometer, which measures the 650–5650 cm⁻¹ region with 0.01 cm⁻¹ spectral resolution [Toon, 1991]. Profiles, obtained at sunrise or sunset, have a vertical resolution of 2–3 km. Systematic errors caused by spectroscopic uncertainties are as large as 12% for stratospheric HNO₃ profiles. Another instrument participating in the Fort Sumner balloon campaigns is the Smithsonian Astrophysical Observatory (SAO) far-infrared spectrometer (FIRS-2), which measures midinfrared and far-infrared thermal emission spectra of a number of stratospheric constituents; in particular, HNO₃ is measured with the ν_9 band between 440 and 470 cm⁻¹ with a systematic uncertainty of ±5% from uncertainties in the ν_9 band strength [Jucks et al., 1999]. As for the MkIV data, vertical resolution is 2–3 km. Finally, the JPL Submillimeterwave Limb Sounder-2 (SLS-2) is a high-resolution heterodyne radiometer-spectrometer that measures limb thermal emission spectra of several species, including HNO₃, at frequencies near 650 GHz. A previous version of the instrument was described by Stachnik et al. [1999]; the newer SLS-2 incorporates an LHe-cooled superconductor insulator superconductor (SIS) quasi-optic mixer that has greater than 20 times the radiometric sensitivity of the earlier Schottky mixer instrument (system temperature T_{sys} of ~250 K double-sideband compared to ~5500 K). Ver-

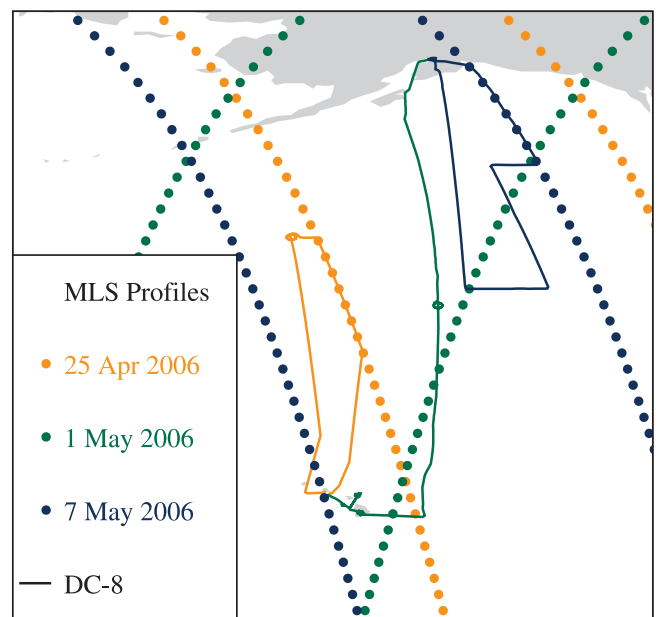


Figure 14. As in Figure 13, for DC-8 flights during the Intercontinental Chemical Transport Experiment–Phase B (INTEX-B) mission conducted from Hawaii and Alaska in April/May 2006.

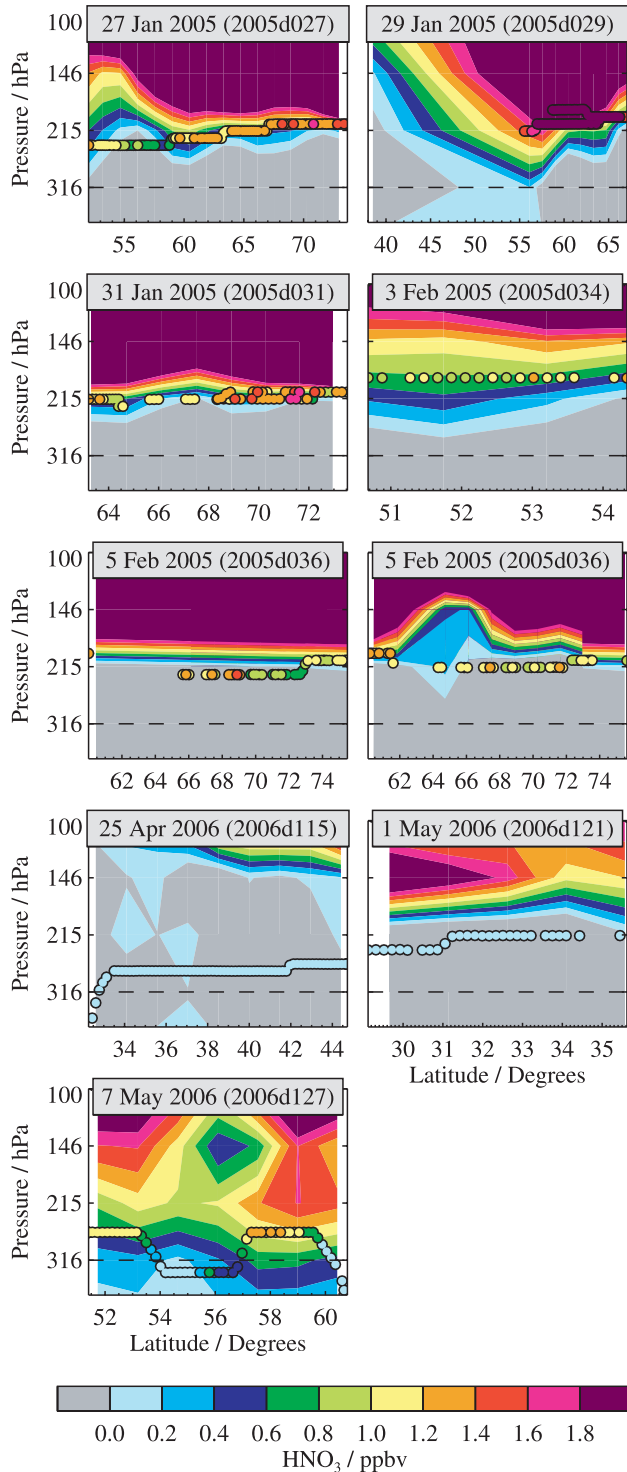


Figure 15. MLS HNO₃ measurements (contours) for 5 d during the PAVE campaign in January/February 2005 and 3d during the INTEX-B campaign in April/May 2006 for which v2.2 data are available. The dashed lines at 316 hPa signify that the MLS data at and below this level are not considered reliable for scientific studies. Overlaid (solid circles) are the SAGA in situ HNO₃ measurements obtained during the portions of the DC-8 flights aligned along Aura ground tracks. Note that the data from the two flight legs on 5 February 2005 are plotted separately since they correspond to different MLS orbits (see Figure 13).

tical resolution of the SLS-2 data is roughly 2–3 km below the balloon float altitude (~ 35 km) and 5–6 km above.

[38] Comparisons between the balloon measurements and coincident MLS measurements for the 2004 and 2005 campaigns are shown in Figures 11 and 12, respectively, where the MLS profiles are within $\pm 1^\circ$ of latitude, $\pm 12^\circ$ of longitude, and ± 12 h of the balloon measurements. Similar comparisons between the 2004 balloon data and v1.5 MLS HNO₃ revealed differences as large as 3 ppbv at the levels surrounding the profile peak, with the magnitude of the discrepancy well outside the combined error bars [Froidevaux *et al.*, 2006]. With the correction of the spectroscopy error (see section 2.6), v2.2 HNO₃ mixing ratios are smaller by $\sim 30\%$, greatly improving the agreement over most of the vertical range. Near the peak of the profiles in 2004, however, v2.2 MLS HNO₃ values are ~ 0.5 –1 ppbv smaller than those from MkIV or FIRS-2. A similar picture emerges from the 2005 intercomparison, with peak MLS values again lower than those from MkIV and FIRS-2 by ~ 0.5 –1 ppbv. The differences are still outside the combined error bars at some levels. Agreement is also poor above 10 hPa in both years and at 100 hPa in 2005, where the MLS mixing ratios are strongly negative. Measurements from SLS-2 (available only for the 2005 campaign) lie between those of MLS and the infrared sensors throughout most of the profile.

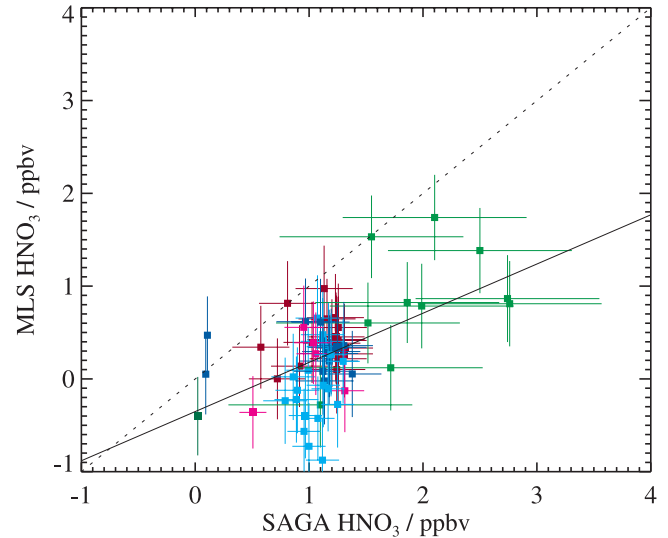


Figure 16. Composite of all available v2.2 MLS HNO₃ measurements and SAGA in situ data obtained during the portions of the DC-8 flights aligned along Aura ground tracks from both the PAVE and INTEX-B campaigns. Symbols represent individual MLS values (y axis) compared to the average of nearby in situ observations (x axis, see text) at 215 hPa, color-coded by flight as in Figures 13 and 14. Vertical error bars show the estimated precision of the MLS HNO₃; horizontal error bars depict the maximum standard deviation of the SAGA data within any of the boxes at a given pressure level for a given flight (see text). The least-squares linear fit to the data is shown by the solid line (number of points = 64, correlation coefficient = 0.53, and slope = 0.53), with the one-to-one line shown dotted.

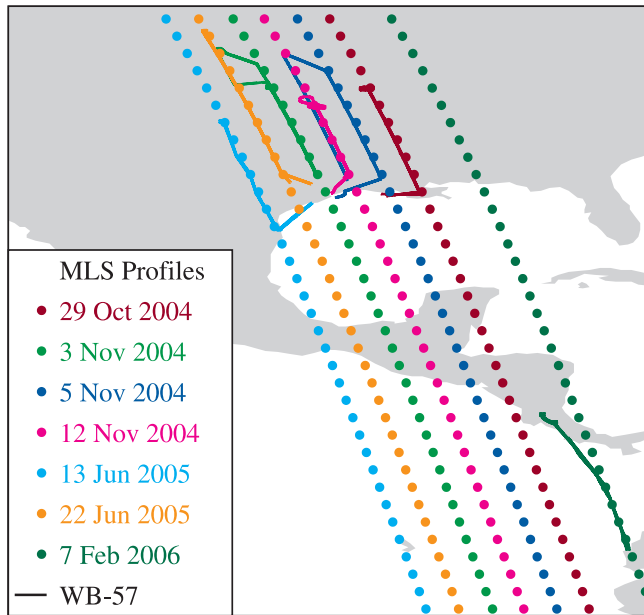


Figure 17. Flight tracks (lines color-coded by date) of the NASA WB-57 high-altitude aircraft during the Aura Validation Experiment (AVE) missions based near Houston, Texas, in October/November 2004 and June 2005 and the Costa Rica AVE (CR-AVE) mission in February 2006. Only flights on days for which both MLS v2.2 and CIMS data are available are shown. The closest MLS ground tracks on these days are indicated by solid dots in corresponding colors.

4.3. Aircraft Measurements

[39] Several aircraft campaigns have been conducted since the launch of Aura; although they have had strong science components, a significant focus of these campaigns has also been to collect observations to assist in the validation of Aura measurements. In situ HNO₃ measurements were made on flights of the NASA DC-8 research aircraft within and on the edge of the Arctic polar vortex as part of the Polar Aura Validation Experiment (PAVE) in January/February 2005. Similar measurements were made from the same aircraft in the Northern Pacific during the Intercontinental Chemical Transport Experiment–Phase B (INTEX-B) mission in April/May 2006. In addition, in situ measurements of HNO₃ in the tropical upper troposphere and lower stratosphere were obtained from the NASA WB-57 high-altitude aircraft during the Aura Validation Experiment (AVE) missions based near Houston, Texas, in October/November 2004 and June 2005 and the Costa Rica AVE (CR-AVE) mission in January/February 2006.

4.3.1. UNH SAGA

[40] The University of New Hampshire (UNH) Soluble Acidic Gases and Aerosols (SAGA) instrument makes in situ measurements of HNO₃ with mist chamber samplers and near-real-time ion chromatographic analysis [Scheuer et al., 2003]. During both the PAVE and INTEX-B campaigns, flights of the NASA DC-8 aircraft were coordinated to align along Aura instrument ground tracks near the time of the satellite overpass, as illustrated in Figures 13 and 14. Note, however, that some of these flights were targeted toward

validation of data from other Aura instruments; in these cases, the aircraft flight tracks are offset from those of MLS. The SAGA measurements of HNO₃ made in the lowermost stratosphere under the Arctic vortex during PAVE have been reported by Dibb et al. [2006].

[41] Using SAGA data for MLS validation purposes raises the issue of how to meaningfully compare the considerably coarser-resolution and less precise satellite measurements, which represent “average” conditions over

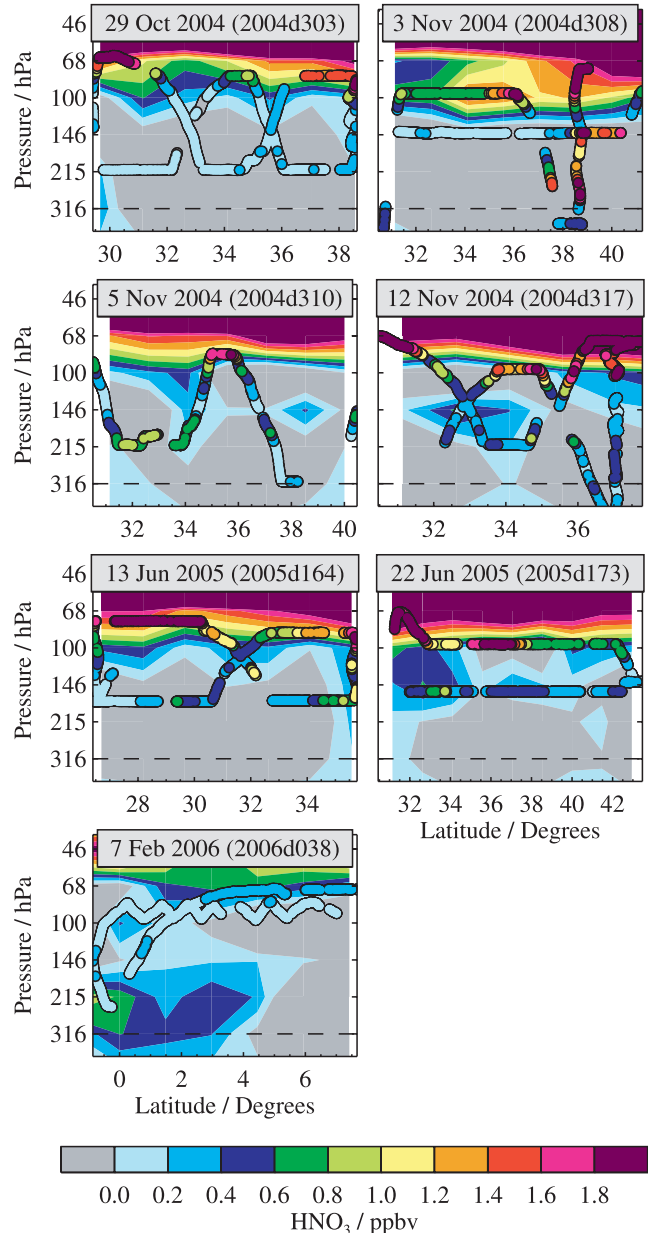


Figure 18. MLS HNO₃ measurements (contours) for 4 d during the AVE campaign in October/November 2004, 2 d during the AVE campaign in June 2005, and 1 d during the CR-AVE campaign in February 2006 for which v2.2 data are available. The dashed lines at and below this level are not considered reliable for scientific studies. Overlaid (solid circles) are the CIMS in situ HNO₃ measurements obtained during the portions of the WB-57 flights aligned along Aura ground tracks.

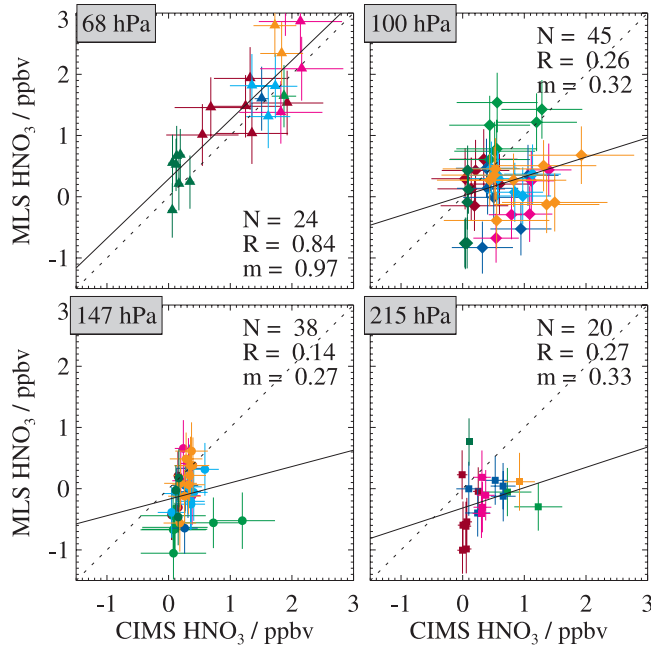


Figure 19. Composite of all available v2.2 MLS HNO₃ measurements and CIMS in situ data obtained during the portions of the WB-57 flights aligned along Aura ground tracks during the AVE and CR-AVE campaigns. Symbols represent individual MLS values (y axes) compared to the average of nearby in situ observations (x axes, see text) at the 68, 100, 147, and 215 hPa pressure levels, color-coded by flight as in Figure 17. Vertical error bars show the estimated precision of the MLS HNO₃; horizontal error bars depict the maximum standard deviation of the CIMS data within any of the boxes at a given pressure level for a given flight (see section 4.3.1). The least-squares linear fit to the data at each level is shown by the solid line (the number of points, N, correlation coefficient, R, and slope, m, are noted in each panel), with the one-to-one line shown.

a relatively large volume of air, with the highly precise in situ measurements, which represent conditions at a local point. Geophysical variability inevitably complicates interpretation of the comparison of data sets having sampling volumes of such vastly different scales. In Figure 15 we take a qualitative approach in which the in situ measurements are simply overlaid on the MLS HNO₃ field most closely coincident to the DC-8 track geographically and temporally. Results are generally encouraging for the MLS retrievals at 215 hPa. SAGA frequently senses fine-scale structure not observable by MLS, but for most flights the spatial trends are roughly in agreement, although MLS mixing ratios appear to be low relative to those recorded by SAGA. It is also tempting to interpret the results for the INTEX-B flight on 7 May 2006 as suggesting that the MLS retrievals at 316 hPa may be useful, but the agreement seen in Figure 15 for this day is probably fortuitous. As discussed in section 2, MLS data are not recommended for scientific use below 215 hPa, where very little independent information is provided by the measurements and the retrieved mixing ratios are often strongly negative.

[42] A quantitative comparison is shown in Figure 16. For these comparisons, all SAGA measurements falling within a

specified interval centered on each individual MLS point are averaged together. The “box” encompassing the SAGA measurements associated with each MLS data point is 1.5° great circle angle (~165 km) wide in the horizontal and one MLS retrieval grid increment (1/6 of a decade in pressure) in the vertical. The extent to which the multiple aircraft observations within a “box” are representative of the average mixing ratio in that box (the quantity most comparable to individual MLS observations) is hard to quantify, as the amount of atmospheric variability throughout the box is unknown. Simply taking the standard deviation of the in situ data within the box would lend undue weight to those cases where the aircraft sampled only a small fraction of the box. Instead, the uncertainty reported (shown by the horizontal error bars in Figure 16) is the largest standard deviation (i.e., variability) seen by the aircraft within any of the boxes at a given pressure level for a given flight.

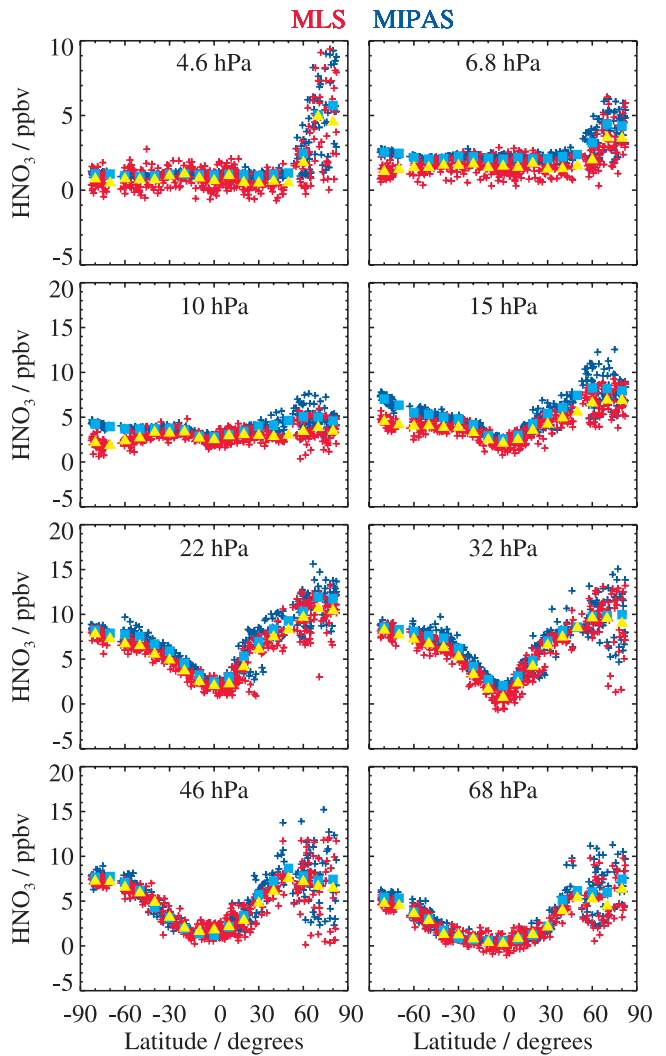


Figure 20. Scatterplot of coincident HNO₃ profiles from MLS v2.2 data (red) and MIPAS data from off-line Oxford retrievals (blue, see text) for 28 January 2005, as a function of latitude for eight selected retrieval surfaces. Overplotted are the zonal mean values calculated in 10°-wide latitude bands for both the MLS (yellow triangles) and MIPAS (cyan squares) data.

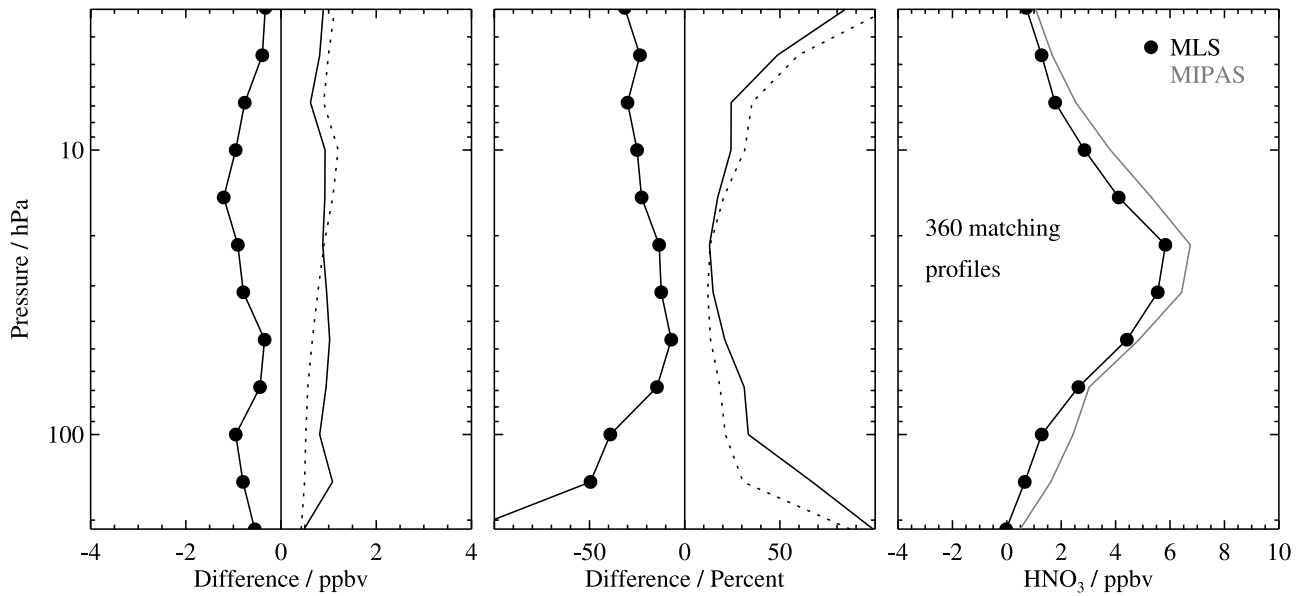


Figure 21. Comparison of coincident HNO₃ profiles from MLS v2.2 data and MIPAS data from off-line Oxford retrievals (see text). (left) Absolute differences (MLS-MIPAS). The black line with dots (symbols indicate MLS retrieval surfaces) shows mean differences, the solid line shows the standard deviation about the mean differences, and the dotted line shows the root sum square of the theoretical precisions of the two data sets. (middle) Same, for percent differences, where percentages have been calculated by dividing the mean differences by the global mean MIPAS value at each surface. (right) Global mean profiles for MLS (black, with dots) and MIPAS (grey).

Again, despite a fair amount of scatter, the degree of agreement lends confidence in the scientific usefulness of the MLS retrievals at 215 hPa, although the MLS data at this level are consistently lower than those observed by SAGA. These comparisons have focused on individual MLS data points; however, as discussed in section 2.4, because of the inherently noisy nature of the MLS HNO₃ data, particularly at the lowest retrieval levels, it will be necessary for most scientific studies using the 215 hPa measurements to perform some latitudinal and/or temporal averaging.

4.3.2. NOAA CIMS

[43] In situ measurements of HNO₃ were made with the NOAA chemical ionization mass spectrometer (CIMS) [Neuman et al., 2001] onboard the NASA WB-57 high-altitude aircraft during several recent missions, including the AVE and CR-AVE campaigns. The CIMS instrument measures HNO₃ using two separate sampling inlets; the forward facing inlet is sensitive to both gas phase and particulate HNO₃, whereas the downward facing inlet is sensitive primarily to gas phase HNO₃ [e.g., Popp et al., 2004]. In performing comparisons with MLS data, we consider only the gas phase HNO₃ CIMS measurements. The CIMS HNO₃ measurements are reported as 1-s averages, with an accuracy of $\pm 25\%$ +40 pptv and a $1-\sigma$ precision of ± 40 pptv.

[44] During both the AVE and CR-AVE campaigns, aircraft flights were coordinated to align with Aura ground tracks near the time of the satellite overpass, providing significant overlap between the in situ- and MLS-observed air masses (Figure 17). Because the same resolution issues arise as for the comparisons between MLS and SAGA data, we take the same approach as in the previous section. Figure 18 shows a qualitative comparison between CIMS

data and the MLS HNO₃ measurements most closely coincident geographically and temporally to the aircraft track. Again, the in situ measurements reveal fine-scale structure that is not observable by MLS, but in most cases the overall spatial trends are roughly in agreement. The WB-57 is capable of attaining much higher altitudes than the DC-8, allowing comparisons with MLS data up to 68 hPa. Throughout much of the vertical domain, except at 68 hPa, MLS values frequently appear to be slightly smaller than those observed by CIMS. This is confirmed by the quantitative comparisons of Figure 19, for which all CIMS measurements falling within a specified interval centered on each individual MLS point are averaged together in the manner described in connection with Figure 16. As before, a significant amount of scatter is seen in these comparisons, and it is difficult to draw definitive conclusions from relatively few coincidences of measurements with such disparate sampling volumes and precisions. Nevertheless, we find the results of Figure 19 encouraging. In particular, the comparison of stratospheric air masses at 68 hPa shows quite good agreement; also notable is the tight clustering of points near zero for both MLS and CIMS at 147 hPa, a region of the atmosphere characterized by relatively uniformly low HNO₃ abundances and small HNO₃ gradients. We judge the MLS HNO₃ retrievals in the upper troposphere and lowermost stratosphere to be useful for scientific studies (typically with some averaging).

4.4. Satellite Measurements

[45] Satellite measurements provide the opportunity for more spatially and temporally extensive intercomparisons than those with ground-based, balloon, or aircraft data sets. They are also typically well matched to the MLS horizontal

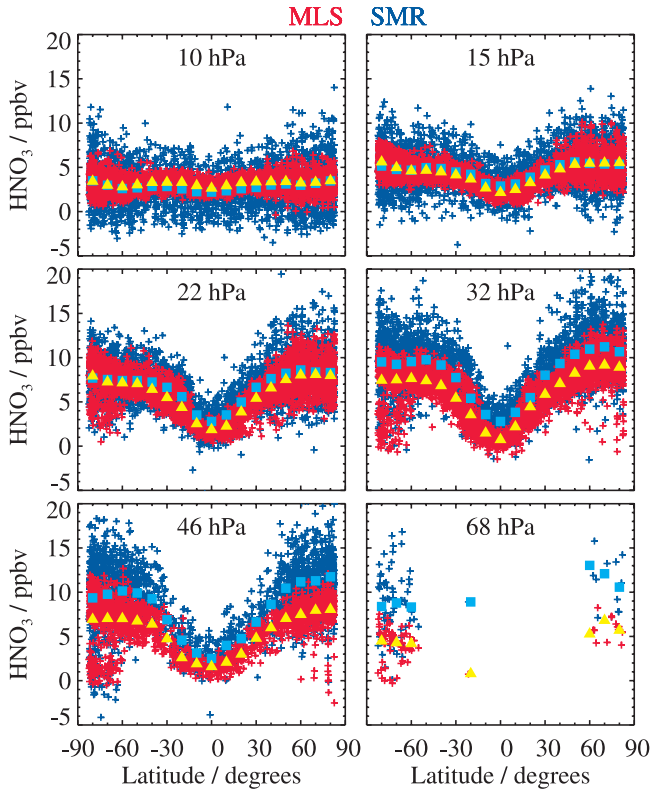


Figure 22. As in Figure 20, for all coincident profiles from 49 d for which Odin/SMR Chalmers version 2.0 and MLS v2.2 HNO₃ measurements are available.

and vertical resolution. Measurements of HNO₃ contemporaneous with those from Aura MLS are available from three other satellite instruments.

4.4.1. MIPAS

[46] The Michelson Interferometer for Passive Atmospheric Sounding (MIPAS) on the European Space Agency

(ESA) Environmental Satellite (Envisat) is a high-resolution infrared limb-sounding Fourier transform spectrometer, measuring HNO₃ from bands near 11.5 μm (870 cm^{-1}) [Fischer and Oelhaf, 1996]. MIPAS operations were suspended in March 2004 because of instrumental anomalies; operations resumed in January 2005 with degraded spectral resolution and a modified duty cycle and scan sequence to extend instrument lifetime [Raspollini et al., 2006; Piccolo and Dudhia, 2007]. The horizontal along-track sampling interval of the MIPAS measurements in the nominal reduced resolution mode is \sim 410 km, and the vertical sampling is \sim 1.5–4 km. The ESA near-real-time operational retrievals are described by Raspollini et al. [2006], and validation of the operational MIPAS HNO₃ profiles and their associated precision are discussed by Mencaraglia et al. [2006], Wang et al. [2007b], and Piccolo and Dudhia [2007]. The ESA operational retrievals use a dedicated MIPAS spectroscopic database that includes recently updated HNO₃ line strengths [Flaud et al., 2006]; use of the revised spectroscopic information results in increases in the retrieved HNO₃ mixing ratios of 13–14% over those obtained using the HITRAN 2000 database [Mencaraglia et al., 2006; Wang et al., 2007a].

[47] In addition to the ESA operational retrievals, several off-line MIPAS data processing systems have been developed at other institutions [e.g., Wang et al., 2007a]. Here we show comparisons with off-line HNO₃ retrievals from algorithms developed at the University of Oxford (A. Dudhia and C. Waymark, personal communication, 2006), funded by the Envisat Calibration/Validation Program. The MIPAS profiles were supplied with a cloud flag for data screening. Like the operational processing, the Oxford retrievals employ the updated MIPAS spectroscopic database. Figures 20 and 21 compare all coincident profiles obtained within $\pm 1^\circ$ in latitude, $\pm 4^\circ$ in longitude, and ± 12 h from nine orbits of MIPAS data collected on 28 January 2005. Agreement in the general morphology of the HNO₃ distribution is excellent, but some significant differences are

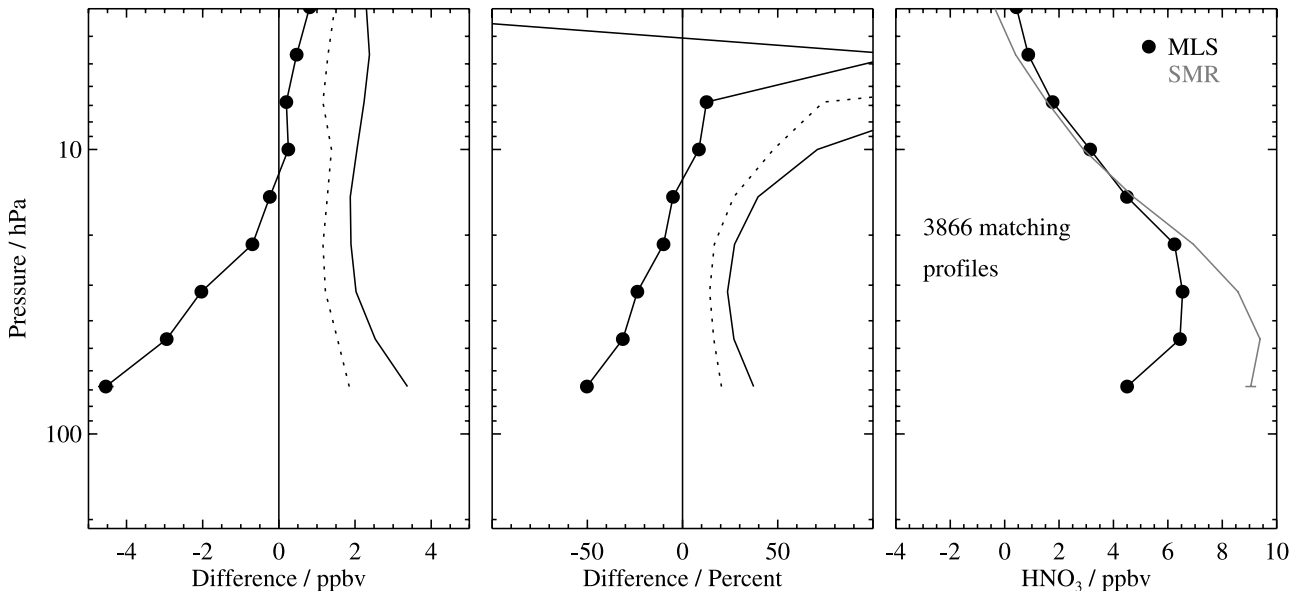


Figure 23. As in Figure 21, for all coincident profiles from 49 d for which Odin/SMR Chalmers version 2.0 and MLS v2.2 HNO₃ measurements are available.

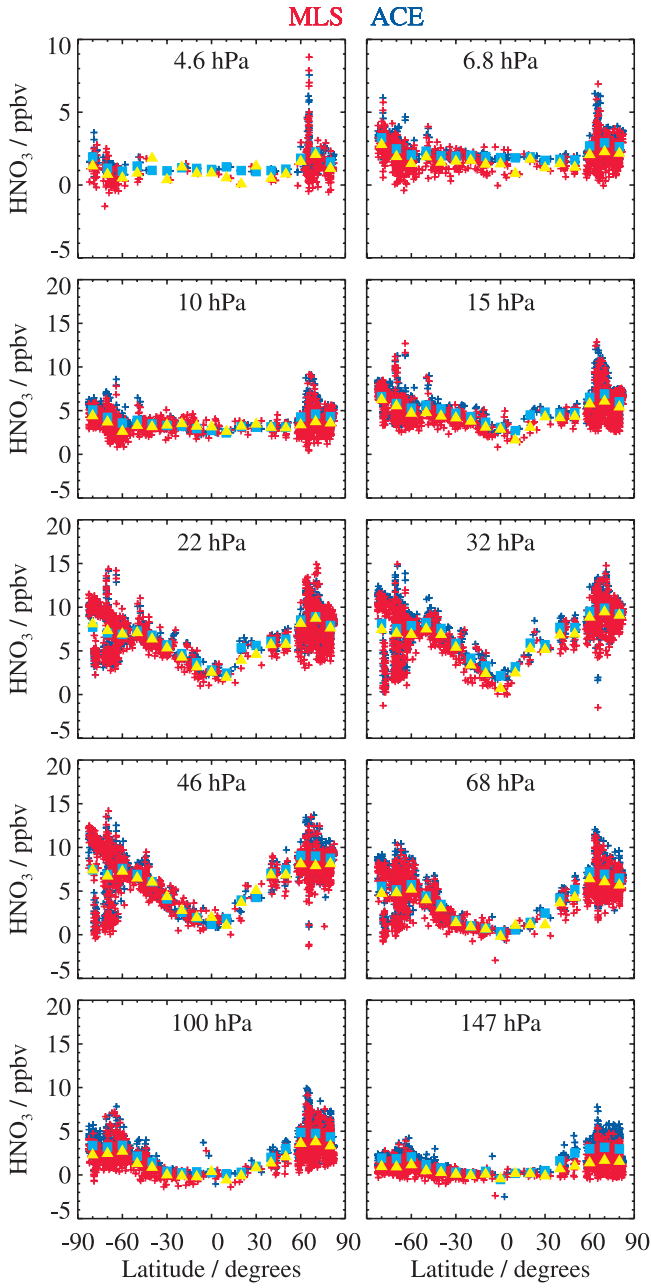


Figure 24. As in Figure 20, for all coincident ACE-FTS version 2.2 and MLS v2.2 HNO₃ measurements (see text).

seen. The scatterplots of Figure 20 show that, although MLS HNO₃ is systematically low relative to that from MIPAS, departures tend to be slightly larger at higher latitudes. The end of January 2005 was a particularly cold period in the Arctic, with extensive polar stratospheric cloud (PSC) formation [e.g., Jimenez et al., 2006]; both MIPAS and MLS record low mixing ratios indicative of HNO₃ sequestration in PSCs in the lower stratosphere, but MLS abundances are considerably smaller. Both instruments also detect a substantial HNO₃ enhancement at northern high latitudes at the topmost levels, but it is less pronounced in the MLS data. Similar high-altitude maxima arising from solar storm activity have been reported previously in

MIPAS data [Orsolini et al., 2005; Stiller et al., 2005]. Figure 21 shows that, on average, differences between MLS and MIPAS HNO₃ values are \sim 10–30% (\sim 0.5–1.0 ppbv) throughout most of the profile, with the standard deviation of the differences of similar magnitude except at the extremes of the vertical range, where very low mixing ratios magnify the percentage deviations.

4.4.2. Odin/SMR

[48] The Swedish-led Odin satellite was launched in February 2001 into a near-polar, Sun-synchronous, \sim 600-km altitude orbit with an 1800 LT ascending node [Murtagh et al., 2002]. Odin operates in a time-sharing arrangement, alternating between astronomy and aeronomy modes; the Submillimetre Radiometer (SMR) observes limb thermal emission from HNO₃ on roughly two measurement days per week using an autocorrelator spectrometer centered at 544.6 GHz. Operational Level 2 HNO₃ retrievals are produced by the Chalmers University of Technology (Göteborg, Sweden). The retrieval methodology and error characterization for the Chalmers version 1.2 data are presented in detail by Urban et al. [2005]; here we use Chalmers version 2.0 HNO₃ data, which have horizontal resolution of \sim 300–600 km, vertical resolution of 1.5–2 km, and single-scan precision better than 1.0 ppbv over the range 18 to 45 km [Urban et al., 2005, 2006; Barret et al., 2006]. The total systematic error is less than 0.7 ppbv throughout the vertical range [Urban et al., 2005, 2006]. Only good quality SMR data points are included in these comparisons (i.e., assigned flag QUALITY = 0, and a measurement response for each retrieved mixing ratio larger than 0.75 to ensure that the information has been derived from the measurements, with a negligible contribution from the climatological a priori profile [Urban et al., 2005; Barret et al., 2006]). Comparisons of Chalmers version 2.0 HNO₃ data with v1.5 MLS HNO₃ data [Barret et al., 2006] and an off-line MIPAS HNO₃ retrieval [Wang et al., 2007a] indicate an altitude shift between matched profiles of \sim 1.5–2 km, probably arising from a systematic error in the simultaneous pointing and temperature/pressure retrieval from the SMR 544.6 GHz band.

[49] Figures 22 and 23 compare all coincident profiles obtained within $\pm 1^\circ$ in latitude, $\pm 4^\circ$ in longitude, and ± 12 h from 49 d for which both SMR and v2.2 MLS data are available. All seasons are represented in this set of comparison days. Although the SMR HNO₃ data appear to be noisier than those from MLS, the scatterplots of Figure 22 indicate very good agreement in the general morphology of the HNO₃ distribution, including a strong feature of HNO₃ depletion in the Antarctic and a weaker signature in the Arctic. Evidence of the SMR altitude shift is seen in these comparisons as well, with MLS low relative to SMR by \sim 0.5–4.5 ppbv (10–50%) below 15 hPa and high relative to SMR by \sim 0.5 ppbv (\sim 10%) above that level (Figure 23). Regardless of the pointing offset, however, it is clear from these results that peak MLS HNO₃ mixing ratios are significantly smaller than those measured by SMR.

4.4.3. ACE-FTS

[50] The Atmospheric Chemistry Experiment Fourier Transform Spectrometer (ACE-FTS) on the Canadian Space Agency's SCISAT-1 mission measures high spectral resolution (0.02 cm^{-1}) solar occultation spectra over the range $750\text{--}4400 \text{ cm}^{-1}$ (2.2 to $13.3 \mu\text{m}$) [Bernath et al., 2005].

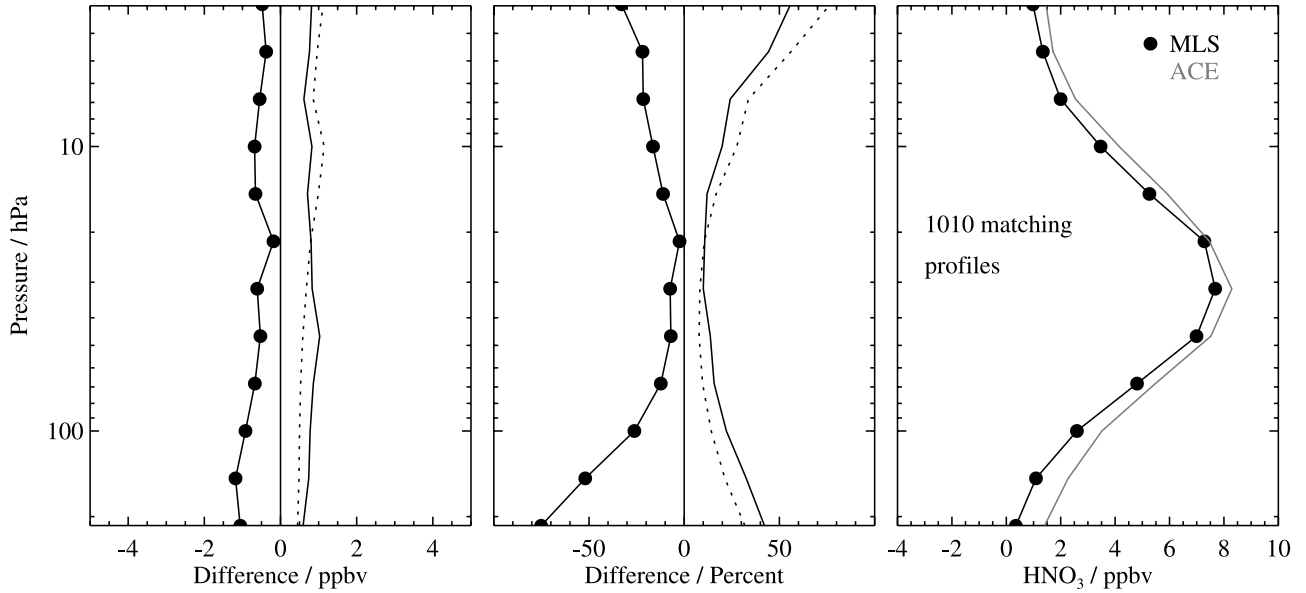


Figure 25. As in Figure 21, for all coincident ACE-FTS version 2.2 and MLS v2.2 HNO₃ measurements (see text).

Vertical profiles are retrieved for as many as 15 sunrises and 15 sunsets per day, the latitudes of which vary over an annual cycle, allowing coverage from 85°S to 85°N with an emphasis on the polar regions during winter and spring. Here we use ACE-FTS version 2.2 data [Boone *et al.*, 2005]. Vertical and horizontal resolution of the ACE-FTS measurements are 3–4 km and ∼500 km, respectively. The HNO₃ retrieval is based primarily on a set of microwindows covering the 1690–1730 cm⁻¹ spectral range, with additional microwindows in the range 860–880 cm⁻¹ used for measurements in the upper troposphere. Typical precision is 2–3%.

[51] In light of the relatively sparse sampling of the occultations, ACE-FTS measurements from days adjacent to those for which v2.2 MLS data are available are also considered in order to augment the number of matched profiles and extend the geographic range of the comparisons. Figures 24 and 25 compare all coincident profiles obtained within ±1° in latitude, ±8° in longitude, and ±12 h from all days for which both ACE and v2.2 MLS data are available. All seasons are represented in this set of comparison days. Similar comparisons between ACE-FTS and v1.5 MLS HNO₃ data indicated a high bias in the MLS measurements of 2–3 ppbv (∼30%) [Froidevaux *et al.*, 2006], attributable to a spectroscopy error as discussed in previous sections. This error has been corrected in v2.2, and MLS HNO₃ values are now slightly lower than those from ACE-FTS but agree to within 0.5–1 ppbv on average, corresponding to ∼10% in much of the stratosphere and to ∼30% everywhere except at the bottom two levels, where average mixing ratios are very low.

[52] Additional analyses in equivalent latitude/potential temperature space comparing HNO₃ observed by ACE-FTS and MLS over the January–March 2005 period as well as several other multiday intervals are shown in a companion paper by Manney *et al.* [2007]. These analyses confirm that

the overall agreement in the morphology and timing of observed features in the two data sets is excellent.

5. Summary and Conclusions

[53] We have assessed the quality and reliability of the Aura MLS version 2.2 (v2.2) HNO₃ measurements. The HNO₃ in v2.2 has been greatly improved over that in the previous version (v1.5); in particular, the profiles are considerably smoother and less oscillatory, unrealistic behavior at the lowest retrieval levels is substantially reduced, and a high bias caused by an error in one of the spectroscopy files used in v1.5 processing has been corrected.

[54] The MLS v2.2 HNO₃ data are scientifically useful over the range 215 to 3.2 hPa. The standard HNO₃ product is derived from the 240-GHz retrievals at and below (i.e., at pressures equal to or larger than) 10 hPa and from the 190-GHz retrievals above that level. A summary of the precision and resolution (vertical and horizontal) of the v2.2 HNO₃ measurements as a function of altitude is given in Table 2.

[55] The impact of various sources of systematic uncertainty has been quantified through a comprehensive set of retrieval simulations. The dominant sources of uncertainty have been shown to be interband pointing offsets, gain compression, contamination from possible errors in ozone, retrieval numerics, and the presence of thick clouds. Table 2 includes estimates of the aggregate potential biases and scaling errors in the measurements compiled from this uncertainty analysis. The overall uncertainty for an individual data point is determined by taking the root sum square (RSS) of the precision, bias, and scaling error terms (for averages, the single-profile precision value is divided by the square root of the number of profiles contributing to the average).

Table 2. Summary of Aura MLS v2.2 HNO₃ Characteristics

Pressure, hPa	Resolution, Vertical × Horizontal, ^a km	Precision, ^b ppbv	Bias Uncertainty, ^c ppbv	Scaling Uncertainty, ^c %	Comments
2.1–0.001	-	-	-	-	unsuitable for scientific use
6.8–3.2	4–5×300	±0.7	±0.5	±10–15%	
22–10	4.5–5.5×450–550	±0.7	±1–2	±10%	
100–32	3.5×400	±0.7	±0.5–1	±5–10%	
147	3.5×400	±0.7	±0.5	±15%	
215	4×500	±0.7	±1	~±30%	
316	-	-	-	-	unsuitable for scientific use
1000–464	-	-	-	-	not retrieved

^aHorizontal resolution in along-track direction; cross-track resolution is ~10 km, and the separation between adjacent retrieved profiles along the measurement track is 1.5° great circle angle (~165 km).

^bPrecision on individual profiles, determined from observed scatter in the data in a region of minimal atmospheric variability.

^cValues should be interpreted as 2- σ estimates of the probable magnitude.

[56] Comparisons with correlative data sets from a variety of different platforms have also been undertaken. A consistent picture emerges that, relative to HNO₃ measurements from ground-based, balloon-borne, and satellite instruments operating in both the infrared and microwave regions of the spectrum, MLS v2.2 HNO₃ mixing ratios are uniformly low by 10–30% throughout most of the stratosphere. The degree of agreement indicated by these comparisons is generally in line with the aggregate uncertainty in the v2.2 MLS HNO₃ measurements (based on the systematic error analysis), given the accuracies of the correlative data sets. Comparisons with in situ measurements made from the DC-8 and WB-57 aircraft in the upper troposphere and lowermost stratosphere indicate that the MLS HNO₃ values are biased low in this region as well.

[57] Quality control should be implemented in any scientific studies using the MLS HNO₃ measurements. Several diagnostics for evaluating data quality are provided along with the retrieved mixing ratios in the MLS Level 2 files. More detail on these quantities is given in section 2.2. Briefly, any data point for which any of the following conditions are met should be discarded: (1) the associated precision value is negative, (2) “Status” is an odd number, (3) “Quality” is less than 0.4, or (4) “Convergence” is greater than 1.8. In addition, nonzero but even values of “Status” indicate that the profile has been marked as questionable, typically because the measurements may have been affected by the presence of thick clouds. It is recommended that at and below 100 hPa all profiles with nonzero values of “Status” be used with extreme caution or discarded altogether because of the potential for cloud contamination.

[58] Validation of satellite measurements is an ongoing process. It is important to continue to evaluate the quality of the MLS HNO₃ data set, especially in light of future refinements to the data processing software. A goal of planned Version 3 algorithms is to reduce the oscillations in the vertical profile and minimize the impact of thick clouds on the retrievals to further improve the HNO₃ measurements in the upper troposphere and lowermost stratosphere. The analyses presented here can be extended as more v2.2 data become available; at the time of writing (February 2007), fewer than 100 d of MLS data have been reprocessed to v2.2. Recent balloon flights from Kiruna, Sweden during the January/February 2007 campaign, continuing satellite missions, and planned deployments of various instruments

during the upcoming International Polar Year, will all afford more opportunities for cross comparisons.

[59] **Acknowledgments.** We are very grateful to the MLS instrument and data operations and development team for their support through all the phases of the MLS project, in particular D. Flower, G. Lau, J. Holden, R. Lay, M. Loo, D. Miller, B. Mills, S. Neely, G. Melgar, A. Hanzel, M. Echeverri, E. Greene, A. Mousessian, C. Vu, and X. Sabounchi. We greatly appreciate the efforts of Bojan Bojkov and the Aura Validation Data Center (AVDC) team, whose work facilitated the MLS validation activities. Thanks to the Aura Project for their support throughout the years (before and after Aura launch), in particular M. Schoeberl, A. Douglass (also as cochair of the Aura validation working group), E. Hilsenrath, and J. Joiner. We also acknowledge the support from NASA Headquarters: P. DeCola for MLS and Aura, and M. Kurylo, J. Gleason, B. Doddridge, and H. Maring, especially in relation to the Aura validation activities and campaign planning efforts. The aircraft campaigns themselves involved tireless hours from various coordinators, including D. Fahey, E. Jensen, P. Newman, M. Schoeberl, H. Singh, D. Jacob, and R. Friedl, as well as K. Thompson, and others involved with campaign flight management and support. We express our thanks to the Columbia Scientific Balloon Facility (CSBF) for providing operations services for the balloon experiments whose data are used in this work. We are grateful to C. Waymark and A. Dudhia at Oxford University for their provision of and assistance with MIPAS HNO₃ retrievals. Three anonymous referees are thanked for their thoughtful comments. Funding for ACE was provided by the Canadian Space Agency and the Natural Sciences and Engineering Research Council (NSERC) of Canada. Odin is a Swedish-led satellite project funded jointly by the Swedish National Space Board (SNSB), the Canadian Space Agency (CSA), the National Technology Agency of Finland (Tekes) and the Centre National d’Études Spatiales (CNES) in France. The CIMS HNO₃ measurements were supported by the NASA Upper Atmospheric Research Program and the NOAA Atmospheric Chemistry and Climate Program. Work at the Jet Propulsion Laboratory, California Institute of Technology, was done under contract with NASA.

References

- Barret, B., et al. (2006), Intercomparisons of trace gas profiles from the Odin/SMR and Aura/MLS limb sounders, *J. Geophys. Res.*, **111**, D21302, doi:10.1029/2006JD007305.
- Bernath, P. F., et al. (2005), Atmospheric Chemistry Experiment (ACE): Mission overview, *Geophys. Res. Lett.*, **32**, L15S01, doi:10.1029/2005GL022386.
- Bloom, S. C., et al. (2005), The Goddard Earth Observing Data Assimilation System, GEOS DAS Version 4.0.3: Documentation and validation, *NASA Tech. Rep. 104606 V26*.
- Boone, C. D., R. Nassar, K. A. Walker, Y. Rochon, S. D. McLeod, C. P. Rinsland, and P. F. Bernath (2005), Retrievals for the atmospheric chemistry experiment Fourier-transform spectrometer, *Appl. Opt.*, **44**, 7218–7231.
- Butchart, N., and E. E. Remsberg (1986), The area of the stratospheric polar vortex as a diagnostic for tracer transport on an isentropic surface, *J. Atmos. Sci.*, **43**, 1319–1339.
- Crutzen, P. J., M. G. Lawrence, and U. Pöschl (1999), On the background photochemistry of tropospheric ozone, *Tellus, Ser. B*, **51**(1), 123–146.
- de Zafra, R. L., V. Chan, S. Crewell, C. Trimble, and J. M. Reeves (1997), Millimeter wave spectroscopic measurements over the South Pole: 3. The behavior of stratospheric nitric acid through polar fall, winter, and spring, *J. Geophys. Res.*, **102**, 1399–1410.

- Dibb, J. E., E. Scheuer, M. Avery, J. Plant, and G. Sachse (2006), In situ evidence for renitrification in the Arctic lower stratosphere during the polar Aura validation experiment (PAVE), *Geophys. Res. Lett.*, **33**, L12815, doi:10.1029/2006GL026243.
- Fischer, H., and H. Oelhaf (1996), Remote sensing of vertical profiles of atmospheric trace constituents with MIPAS limb-emission spectrometers, *Appl. Opt.*, **35**, 2787–2796.
- Flaud, J.-M., G. Brizi, M. Carlotti, A. Perrin, and M. Ridolfi (2006), MIPAS database: Validation of HNO₃ line parameters using MIPAS satellite measurements, *Atmos. Chem. Phys.*, **6**, 5037–5048.
- Froidevaux, L., et al. (2006), Early validation analyses of atmospheric profiles from EOS MLS on the Aura satellite, *IEEE Trans. Geosci. Remote Sens.*, **44**, 1106–1121.
- Goyette, T., W. Ebenstein, F. De Lucia, and P. Helminger (1988), Pressure broadening of the millimeter and submillimeter wave spectra of nitric acid by oxygen and nitrogen, *J. Molec. Spectrosc.*, **128**, 108–116.
- Jimenez, C. J., H. C. Pumphrey, I. A. MacKenzie, G. L. Manney, M. L. Santee, M. J. Schwartz, R. S. Harwood, and J. W. Waters (2006), EOS MLS observations of dehydration in the 2004–2005 polar winters, *Geophys. Res. Lett.*, **33**, L16806, doi:10.1029/2006GL025926.
- Jucks, K. W., D. G. Johnson, K. V. Chance, W. A. Traub, and R. J. Salawitch (1999), Nitric acid in the middle stratosphere as a function of altitude and aerosol loading, *J. Geophys. Res.*, **104**, 26,715–26,723.
- Kleinböhl, A., et al. (2005), Denitrification in the Arctic mid-winter 2004/2005 observed by airborne submillimeter radiometry, *Geophys. Res. Lett.*, **32**, L19811, doi:10.1029/2005GL023408.
- Livesey, N. J., W. V. Snyder, W. G. Read, and P. A. Wagner (2006), Retrieval algorithms for the EOS Microwave Limb Sounder (MLS), *IEEE Trans. Geosci. Remote Sens.*, **44**, 1144–1155.
- Livesey, N. J., et al. (2007a), Version 2.2 Level 2 data quality and description document, *Tech. Rep. JPL D-32381*, Jet Propul. Lab., Pasadena, Calif. (Available at <http://mls.jpl.nasa.gov>)
- Livesey, N. J., et al. (2007b), Validation of Aura Microwave Limb Sounder O₃ and CO observations in the upper troposphere and lower stratosphere, *J. Geophys. Res.*, doi:10.1029/2007JD008805, in press.
- Manney, G. L., et al. (2007), Solar occultation satellite data and derived meteorological products: Sampling issues and comparisons with Aura MLS, *J. Geophys. Res.*, doi:10.1029/2007JD008709, in press.
- Mencaraglia, F., G. Bianchini, A. Boscaleri, B. Carli, S. Ceccherini, P. Raspollini, A. Perrin, and J.-M. Flaud (2006), Validation of MIPAS satellite measurements of HNO₃ using comparison of rotational and vibrational spectroscopy, *J. Geophys. Res.*, **111**, D19305, doi:10.1029/2005JD006099.
- Murtagh, D., et al. (2002), An overview of the Odin atmospheric mission, *Can. J. Phys.*, **80**, 309–319.
- Muscati, G., M. L. Santee, and R. L. de Zafra (2002), Intercomparison of stratospheric HNO₃ measurements over Antarctica: Ground-based millimeter-wave versus UARS/MLS Version 5 retrievals, *J. Geophys. Res.*, **107(D24)**, 4809, doi:10.1029/2002JD002546.
- Neuman, J. A., et al. (2001), In situ measurements of HNO₃, NO_y, NO, and O₃ in the lower stratosphere and upper troposphere, *Atmos. Environ.*, **35**, 5789–5797.
- Orsolini, Y. J., G. L. Manney, M. L. Santee, and C. E. Randall (2005), An upper stratospheric layer of enhanced HNO₃ following exceptional solar storms, *Geophys. Res. Lett.*, **32**, L12S01, doi:10.1029/2004GL021588.
- Piccolo, C., and A. Dudhia (2007), Precision validation of MIPAS-Envisat products, *Atmos. Chem. Phys.*, **7**, 1915–1923.
- Pickett, H. M., R. L. Poynter, E. A. Cohen, M. L. Delitsky, J. C. Pearson, and H. S. P. Müller (1998), Submillimeter, millimeter, and microwave spectral line catalog, *J. Quant. Spectrosc. Radiat. Transfer*, **60**, 883–890.
- Popp, P. J., et al. (2004), Nitric acid uptake on subtropical cirrus cloud particles, *J. Geophys. Res.*, **109**, D06302, doi:10.1029/2003JD004255.
- Raspollini, P., et al. (2006), MIPAS level 2 operational analysis, *Atmos. Chem. Phys.*, **6**, 5605–5630.
- Read, W. G., Z. Shippoly, M. J. Schwartz, N. J. Livesey, and W. V. Snyder (2006), The clear-sky unpolarized forward model for the EOS Aura Microwave Limb Sounder (MLS), *IEEE Trans. Geosci. Remote Sens.*, **44**, 1367–1379.
- Read, W. G., et al. (2007), Aura Microwave Limb Sounder upper tropospheric and lower stratospheric H₂O and RH validation, *J. Geophys. Res.*, doi:10.1029/2007JD008752, in press.
- Rodgers, C. D. (2000), *Inverse Methods for Atmospheric Sounding: Theory and Practice*, World Sci., Singapore.
- Santee, M. L., G. L. Manney, L. Froidevaux, W. G. Read, and J. W. Waters (1999), Six years of UARS Microwave Limb Sounder HNO₃ observations: Seasonal, interhemispheric, and interannual variations in the lower stratosphere, *J. Geophys. Res.*, **104**, 8225–8246.
- Santee, M. L., G. L. Manney, N. J. Livesey, and W. G. Read (2004), Three-dimensional structure and evolution of stratospheric HNO₃ based on UARS Microwave Limb Sounder measurements, *J. Geophys. Res.*, **109**, D15306, doi:10.1029/2004JD004578.
- Santee, M. L., et al. (2005), Polar processing and development of the 2004 Antarctic ozone hole: First results from MLS on Aura, *Geophys. Res. Lett.*, **32**, L12817, doi:10.1029/2005GL022582.
- Scheuer, E., R. W. Talbot, J. E. Dibb, G. K. Seid, L. DeBell, and B. Lefer (2003), Seasonal distributions of fine aerosol sulfate in the North American Arctic basin during TOPSE, *J. Geophys. Res.*, **108(D4)**, 8370, doi:10.1029/2001JD001364.
- Schoeberl, M. R., et al. (2006a), Chemical observations of a polar vortex intrusion, *J. Geophys. Res.*, **111**, D20306, doi:10.1029/2006JD007134.
- Schoeberl, M. R., et al. (2006b), Overview of the EOS Aura mission, *IEEE Trans. Geosci. Remote Sens.*, **44**, 1066–1074.
- Solomon, S. (1999), Stratospheric ozone depletion: A review of concepts and history, *Rev. Geophys.*, **37**, 275–316.
- Stachnik, R. A., R. Salawitch, A. Engel, and U. Schmidt (1999), Measurements of chlorine partitioning in the winter Arctic stratosphere, *Geophys. Res. Lett.*, **26**, 3093–3096.
- Stiller, G. B., et al. (2005), An enhanced HNO₃ second maximum in the Antarctic midwinter upper stratosphere 2003, *J. Geophys. Res.*, **110**, D20303, doi:10.1029/2005JD006011.
- Swinbank, R., N. B. Ingleby, P. M. Boorman, and R. J. Renshaw (2002), A 3D variational data assimilation system for the stratosphere and troposphere, *Tech. Rep. 71*, Met Off., Exeter, U. K.
- Toon, G. C. (1991), The JPL MkIV interferometer, *Opt. Photon. News*, **2**, 19–21.
- Urban, J., et al. (2005), Odin/SMR limb observations of stratospheric trace gases: Level 2 processing of ClO, N₂O, HNO₃, and O₃, *J. Geophys. Res.*, **110**, D14307, doi:10.1029/2004JD005741.
- Urban, J., et al. (2006), Odin/SMR limb observations of trace gases in the polar lower stratosphere during 2004–2005, in *Proceedings of the ESA First Atmospheric Science Conference, 8–12 May 2006, Frascati, Italy*, edited by H. Lacoste, Eur. Space Agency Spec. Publ., ESA-SP-628.
- Wang, D. Y., et al. (2007a), Validation of nitric acid retrieved by the IMK-IAA processor from MIPAS/ENVISAT measurements, *Atmos. Chem. Phys.*, **7**, 721–738.
- Wang, D. Y., et al. (2007b), Validation of MIPAS HNO₃ operational data, *Atmos. Chem. Phys. Disc.*, **7**, 5173–5251.
- Waters, J. W. (1993), *Microwave limb sounding*, in *Atmospheric Remote Sensing by Microwave Radiometry*, edited by M. A. Janssen, chap. 8, pp. 383–496, John Wiley, New York.
- Waters, J. W., et al. (2006), The Earth Observing System Microwave Limb Sounder (EOS MLS) on the Aura satellite, *IEEE Trans. Geosci. Remote Sens.*, **44**, 1075–1092.
- Zondlo, M., P. Hudson, A. Prenni, and M. Tolbert (2000), Chemistry and microphysics of polar stratospheric clouds and cirrus clouds, *Annu. Rev. Phys. Chem.*, **51**, 473–499.

P. F. Bernath, Department of Chemistry, University of York, York, YO10 5DD, UK.

C. D. Boone, Department of Chemistry, University of Waterloo, 200 University Avenue W., Waterloo, ON, Canada N2L 3G1.

R. E. Cofield, D. T. Cuddy, W. H. Daffer, B. J. Drouin, L. Froidevaux, R. A. Fuller, R. F. Jarnot, B. W. Knosp, A. Lambert, N. J. Livesey, V. S. Perun, W. G. Read, M. L. Santee (corresponding author), W. V. Snyder, R. A. Stachnik, P. C. Stek, R. P. Thurstans, G. C. Toon, P. A. Wagner, and J. W. Waters, Jet Propulsion Laboratory, 4800 Oak Grove Drive, Pasadena, CA 91109, USA. (mls@mls.jpl.nasa.gov)

R. L. de Zafra, Department of Physics and Astronomy, State University of New York, Stony Brook, S138A Physics Building, Stony Brook, NY 11794, USA.

J. E. Dibb, Climate Change Research Center, Institute for the Study of Earth, Oceans, and Space, University of New Hampshire, Morse Hall, 39 College Road, Durham, NH 03824, USA.

D. W. Fahey and P. J. Popp, Chemical Sciences Division, Earth System Research Laboratory, NOAA, Boulder, CO 80305, USA.

K. W. Jucks, Harvard-Smithsonian Center for Astrophysics, Cambridge, MA 02138, USA.

G. L. Manney, Department of Physics, New Mexico Institute of Mining and Technology, Socorro, NM 87801, USA.

T. P. Marcy, 730 N. 23rd Street #300, Milwaukee, WI 53233, USA.

D. Murtagh and J. Urban, Department of Radio and Space Science, Chalmers University of Technology, SE-41296 Göteborg, Sweden.

G. Muscati, Istituto Nazionale di Geofisica e Vulcanologia, Via di Vigna Murata, 605, I-00143 Rome, Italy.

K. A. Walker, Department of Physics, University of Toronto, 60 St. George Street, Toronto, ON, Canada M5S 1A7.